PROCESS MODELING SYSTEM FOR PRESS CURE, CLOSED-CAVITY-TOOLED THICK COMPOSITES

by

ARVEN H. SAUNDERS III

Presented to the Faculty of the Graduate School of

The University of Texas at Arlington in Partial Fulfillment

of the Requirements

for the Degree of

DOCTOR OF PHILOSOPHY

THE UNIVERSITY OF TEXAS AT ARLINGTON

August 2011

Copyright © by Arven H. Saunders III 2011

All Rights Reserved

ACKNOWLEDGEMENTS

This dissertation has taken many years to complete and would not have been possible without the support of many people. My wife Theodora has been my constant advocate and source of strength. I am very grateful for the invaluable support and guidance that Dr. Don Liles, my supervising professor, has provided over these years. I would like to thank my dissertation committee members Dr. Brian Huff, Dr. Panos Shiakolas, Dr. John Priest, and Dr. Jamie Rogers for their interest in my research and their willingness to serve on the committee. I am grateful to numerous teachers, mentors, and colleagues, living or dead, whose inspiration has given me strength, courage and encouragement to do this work, among them Mrs. Whitehead, Mr. Wheeler, Dr. R.R. Boedeker, Dr. B.K. Lambert, Dr. Bob Lange and Dr. Yih-Farn Chen. Finally, I thank my family for their unwavering support.

April 18, 2011

ABSTRACT

PROCESS MODELING SYSTEM FOR PRESS CURE, CLOSED-CAVITY-TOOLED THICK COMPOSITES

Arven H. Saunders, III, PhD

The University of Texas at Arlington, 2011

Supervising Professor: Don Liles

Thick structural composite parts often use press curing with closed-cavity tooling for achieving dimensional tolerances. A commonly encountered defect for these parts is fiber waviness, which limits its structural strength. The yield for such parts often suffers due to trial and error methods used to develop successful cure processes. In addition, yield for these parts suffers due to material variation. The objectives that were accomplished through this research were to: develop and validate a simplified yet practical cure process model for press cured thick composite parts, utilize the model in order to seek time-efficient optimized cure processes, investigate the effects of material variation on optimized cure processes, and to utilize the model to investigate the origins of fiber waviness. The model was found to indicate the conditions under which it is likely that fiber waviness occurs.

TABLE OF CONTENTS

LIST OF ILLUSTRATIONS

LIST OF TABLES

CHAPTER 1

INTRODUCTION

1.1 Background

The employment of composite materials continues to increase, especially for high performance aerospace products. Thick laminates are a class of laminates that are employed for critical applications, such as rotorcraft components (for example, blade spars, flex beams, and yokes) that carry power to the rotor blades. These components are flight-critical, tasked with carrying heavy static and vibratory loads. Because of their stringent dimensional tolerances required, they are most often press cured in closed-cavity tooling. While their design is driven to meet the loads associated with form, fit, and function, manufacturing such components has often proven to be a challenge. Some background on the nature of the fabrication and cure process steps will be presented next. Figure 1.1 summarizes the sequence of major process

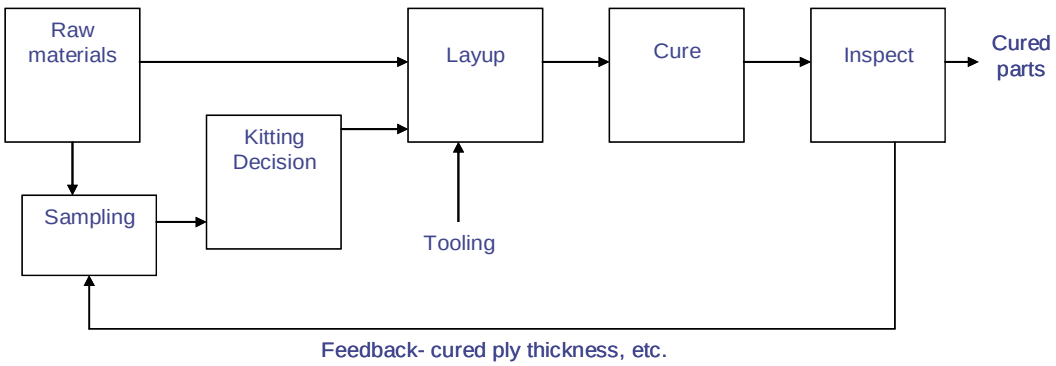

Figure 1.1. Composite Part Fabrication Overview.

steps for fabrication of thick composite laminates. The primary raw materials are preimpregnated composite (prepreg), comprised of (uncured) resin with multiple reinforcing fibers. The most commonly used resin is epoxy, and typical resin content of prepreg is in the range of 33% by weight. The balance of the weight is contributed by high modulus fibers, used

to carry the load. The most commonly used fibers are graphite and fiberglass. Fibers can be oriented in a single direction (unidirectional) or can be woven into a variety of fabrics onto which the resin can be impregnated. Most of the plies in flight-critical thick composites are of unidirectional prepreg material to provide the tensile strength along its length. The multiplicity of fibers held in relative position to each other by the cured resin accounts for the tremendous strength-to-weight advantage of composite material.

The design of a thick composite part specifies a target value or range for the final cured part thickness and weight. It also defines a set of optional plies that can be added to the nominal configuration in the case when the estimated per ply cured thickness is less than the nominal ply thickness; it also specifies certain plies that can be omitted from the layup if the estimated per ply thickness is above the nominal. Kitting specifies exactly which and how many plies will be contained in the laminate.

Properties of the prepreg are tested and evaluated to provide input to the kitting decision. These properties include resin content, fiber areal weight, gel temperature, and estimated ply thickness. However, the actual ply thickness within the cured laminate is stochastic in nature and depends on the cure and consolidation process.

Through the layup process the laminate is built ply by ply, much like each page can be stacked up horizontally to form a book. Although automation of the layup process has been envisioned for a long time, most thick laminates are still layed up by hand. The mechanic lays each ply down, the prepreg resin “tack” or stickiness keeping it stuck to the previous plies in the stack. The bond tool is the vessel that holds the laminate to its desired geometry during layup and cure.

Computer-controlled cure control systems are commonly used to perform a cure cycle recipe of predefined segments comprising temperature and pressure setpoints over time. The combination of heat and pressure over time transforms the laminate into a durable and fatigue-resistant component.

Inspection and evaluation techniques are used to verify that parts are acceptable in relation to the design requirements and specifications. Inspection methods range from visual evaluation to dimensional checks, and nondestructive inspection (NDI). Process engineering is part of the feedback mechanism by interpreting inspection results and making changes as necessary to the process.

1.2 The Nature of the Problem

Due to their superior characteristics, composite materials are increasingly being applied to make thicker and more complex laminate components. The critical roles these laminates are designed to fulfill have translated into more complex fabrication processes with more demanding quality requirements. Thick laminates have subsequently brought with them significant challenges to find cost-effective methods and methodologies to maintain acceptable yields. Although autoclave methods have been used for these laminates, autoclave are limited in pressure available for consolidation. As a result these parts are often press cured within closed-cavity tooling. The chief advantage of press methods is their ability to meet dimensional tolerance requirements and repeatability. However, this advantage is offset by its sensitivity to material variation and thus the variability of its yield.

A representative thick composite part (flexbeam) is illustrated by the simplified schematic in Figure 1.2. The nature of these parts is relatively high thickness and strict dimensional tolerances at attachment locations, separated by relatively thinner part sections, with thickness tapered between these ends of the thickness range. Note that the highest thickness part regions feature many plies that are tapered down to thinner transition areas separating the other thick region. Transition of the thickness is effected by drop-offs or terminations of plies along the length of the laminate. The thickness of such a part could vary from 100 plies (≥ 1”) at the root (thickest) end of the flexbeam, to 30 plies (0.3”) over the center

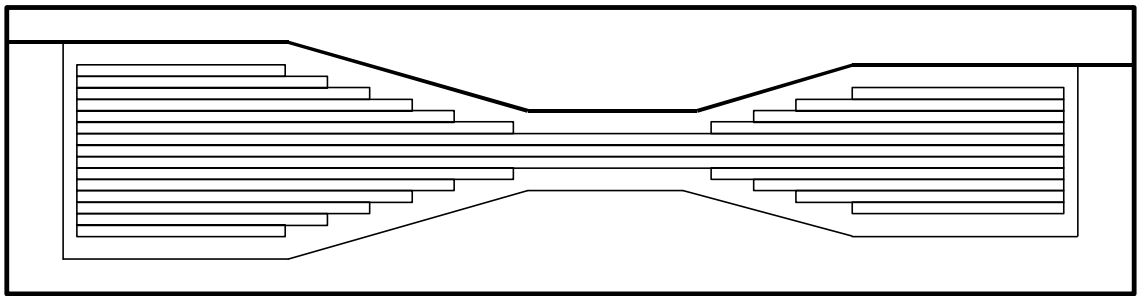

Figure 1.2. Schematic Representation of Thickness for a Typical Thick Laminate (side or through thickness view).

region, and up to 80 plies (0.8") at the other end. Note that the ply drop-offs approximate a smooth tapered ramp. The figure also shows how a closed cavity tool is designed to impose the desired tapered ramp in thickness for the cured laminate.

The most common defects for press cured thick laminates are fiber waviness, porosity, and voids. Fiber waviness, also known as "marcelling" or "fiber wash", is a distortion of the fiber layers in the laminate. Both porosity and voids are inclusions in the cured laminate structure that cannot contribute to its load-carrying capacity. A void is any inclusion of non-resin volume, i.e., open space within the cured laminate; porosity is distinguished by scattered and widely distributed minute water vapor, air, or volatiles within a localized volume of cured resin.

For the earlier generations of epoxy resins (for example, Hercules 3501-6) the predominant quality problems are porosity and voids. With the advent of newer epoxy resins such as Hexcel 8552 and their application to thick composites, a frequent defect has become fiber waviness. There is a limited understanding of this defect and its occurrence is difficult to predict or control. A great deal of work has been conducted to develop improve cure processes to alleviate this defect. Variability in material properties, e.g., ply thickness has also found to be a contributor.

Figure 1.3 displays an example of a thick S2/8552 glass/epoxy laminate section with this defect (from Ng (Ng, 1998, a)). As can be seen in the figure, fiber/layer waviness is a coherent wave linearity with respect to a nominally straight direction. In-plane waviness occurs

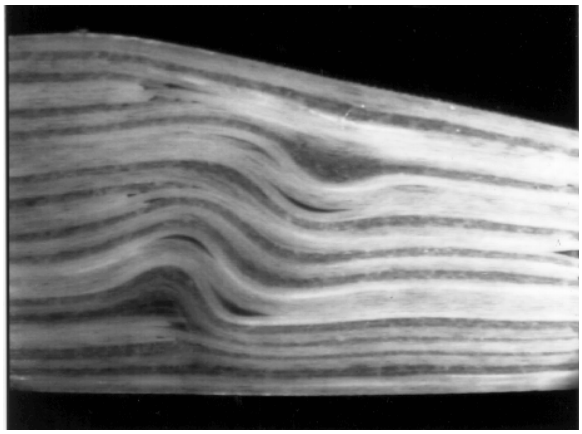

Figure 1.3. Fiber/Layer Waviness in a Section of a Thick S2/8552 Composite Laminate.

within the plane (sideways) of each layed up ply; out-of-plane waviness involves a wave in the thickness direction. This defect has caused great concern in the manufacture of thick tapered section composites for the rotorcraft producers. Extensive testing and analysis has shown that fiber waviness has significant impact on the overall structural integrity of thick laminates. Degradation in compressive strength, fatigue properties, and tensile strength has been reported by various researchers (Adams, 1996). As a result, the tolerance for this nonconformance has been reduced.

To meet these challenges, research and development effort continues in a number of directions. Greater demands have been made of suppliers to reduce material property variation. Designed experimental work has sought to find those aspects of the layup and cure preparation work that are most critical and how better to control them. Because much of composites fabrication involves manual labor, automation has been applied to selected operations such as tape laying, laminate debulk, and fiber placement. More advanced NDI technology has produced greater defect detection capabilities. The composites producers community has also continued its focus on cure cycle improvement and optimization.

1.3 Problem Statement

Thick (at least ½") composite laminates are increasingly employed to applications such as rotorcraft components. Of the many process steps involved in their fabrication, the cure

process is the most critical since it applies the heat and pressure to irreversibly transform the raw material into durable product. Press cure and closed-cavity tooling are a commonly used process approach to ensure part dimensional control. However, the yield for these parts remains variable, thus necessitating additional costs for inspection, testing, and rework.

Typical approaches to process improvement utilize some measure of trial and error methods. Even structured methods, such as designed experiments, entail inefficiency in finding an optimum process, due to the complexity of this problem environment. A comprehensive, validated modeling capability offers the ability to more efficiently investigate the multiple variables involved. The research presented here was directed towards modeling efficient cure cycles with respect to a variety of different constraints.

1.4 Objectives of Research

The objectives of this dissertation were several. The first objective was to develop an integrated physical model of the press cure of thick laminate composites utilizing two different representative material systems. The second objective was to apply the model, once validated, within an optimization scheme to determine the most time-efficient cure cycle processes. A third objective was to utilize the model to investigate the origins of fiber waviness for these thick composite laminates, and then to assess the impact of material variability on fiber waviness.

CHAPTER 2

REVIEW OF RELATED RESEARCH AND LITERATURE

2.1 Cure Process Overview

The approach taken in this research required that the nature of press cure and consolidation for thick composites first be understood. This understanding is coordinated with appropriate process tooling, sensors, and control strategies necessary to ensure part quality. This section presents a survey of research and literature related to the dissertation research work, requiring knowledge and understanding of:

1- unique characteristics and challenges of press molded thick laminates

2- cure cycle development and use of models

3- temperature and resin cure reactions

4- pressure and laminate consolidation

5- cure cycle optimization

6- material and process variability

Composites are formed by in-situ cure (polymerization) of thermosetting polymer matrices (resins) with the fibers. Elevated temperatures are used to initiate and sustain a crosslinking, exothermic, chemical reaction that is the cure reaction. Concurrently, an applied pressure serves to consolidate and expel voids in the composite and volatiles that form during the reaction. The schedule of temperature and pressure change over time is known as the cure cycle. Figure 2.1 illustrates how pressure is applied in coordination with heating during a typical bond press cure cycle recipe. Part temperatures are driven by the higher platen temperatures during heat up; an intermediate dwell is used to ensure temperature consistency within the laminate. Under this condition the resin viscosity decreases and pressure is applied to

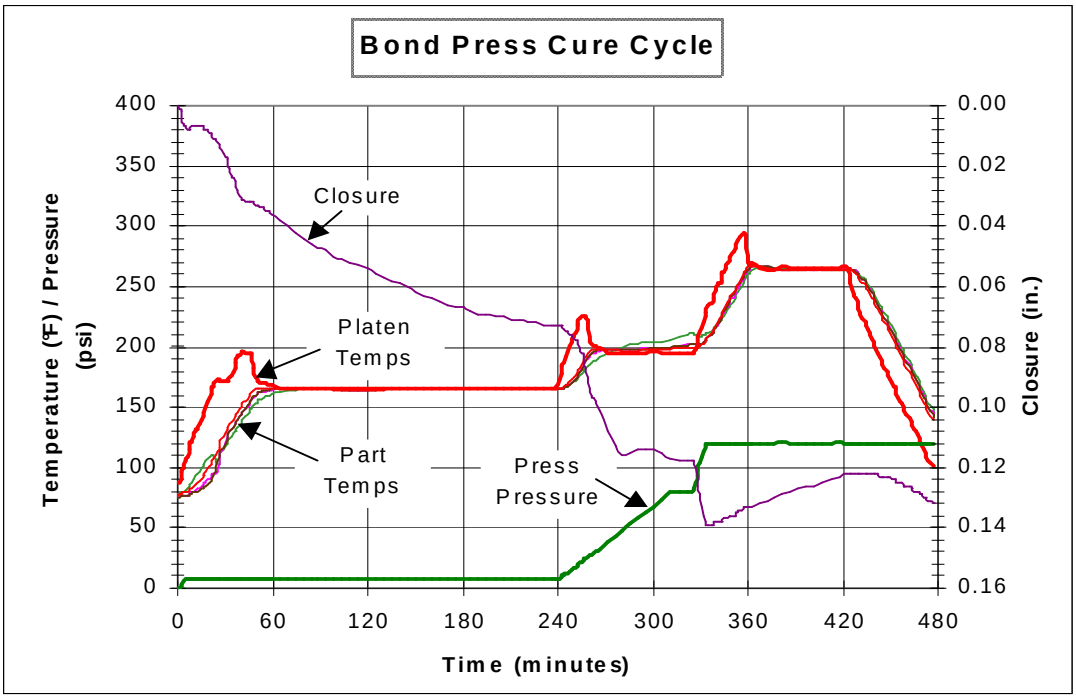

Figure 2.1. A Typical Bond Press Cure Cycle.

consolidate the laminate, suppress voids, and expel volatiles. Following this stage, the temperature is ramped up to the final cure temperature where it is maintained until sufficiently cured. Cool-down brings the part temperature back to ambient and completes the process.

The goals of a successful cure are an efficient process in terms of time and cost, good consolidation with low void volume and a high degree of cure. An optimum process would minimize overall cost while satisfying each requirement. The difficulty in controlling the cure process is to manage the interactions of temperature distribution, degree of cure, laminate thickness, and void content by manipulating only the press temperature and pressure.

2.2 Uniqueness of Thick Laminates

Thick composites pose unique and substantial challenges for cure and consolidation control. Temperature control for these parts is made much more complex due to the number of plies and the effective insulation between the inner and outer plies within the laminate. As heat is applied, the outer plies closely follow the source press temperature, while the innermost plies

greatly lag in temperature. As a result, the conventional approach is to heat a thick laminate very slowly to allow consistency in temperatures through the thickness, thereby lengthening the process time. However, when the cure reaction begins to accelerate, the interior of the laminate generates its own heat from the reaction, outweighing the heat contribution from the external source. At this point, temperature uniformity through the laminate thickness is a balance of the internal and external heat flows. Low conductivity fibers such as fiberglass pose a distinct danger of exotherm (thermal runaway or spike). Thus, the heat-up rate must be controlled, as exotherm is characterized by significant temperature disparity across the laminate thickness that causes major damage to the laminate. The ability to avoid this condition is a function of the thickness and the fiber used.

Closed-cavity tooling is designed to constrain the laminate during the cure to ensure dimensional conformance. Essentially, the closed-cavity tool is comprised of a top and bottom half. The laminate is layed up into the bottom half, then the tool top is located with respect to the bottom, resting on the laminate surface. During the press cure cycle, the heated platens convey a clamping pressure to the tool halves to maintain pressure on the laminate. Gaps are designed into the tool between the top/bottom and the sides to allow a path for resin bleed during the cycle.

While press curing and tooling has the advantage of dimensional repeatability, it is more frequently associated with the defect of fiber waviness. As mentioned in Chapter 1, this defect has a major impact on part strength properties. The source or origin of this defect is not fully understood but several researchers have postulated that it is linked to the occurrence of local or microbuckling of the prepreg due to compressive stresses encountered during cure, e.g, Chun et al (Chun, 2000) and Jochum (Jochum, 2003). The present research was aimed at further exploring the underlying mechanisms of this defect.

2.3 Cure Cycle Development

Cure cycle development for a thick laminate is a knowledge-intensive process involving substantial amounts of trial and error. Lab test and analyses are conducted to characterize the resin polymer to be cured, and quantify the changes in resin state (reaction status and viscosity) that take place with temperature changes. Process models are built based on these test data and incorporated within the knowledgebase. Since these instruments use only a small material sample, larger more representative subscale production articles are used to explore fabrication methods and tooling. Experts of the material system iterate on candidate cure cycles, using inspection and test results from the cured laminate as guidance. To validate the cure process as acceptable, a series of non-destructive and destructive tests is conducted.

Once a workable cycle has been defined, computerized systems are used to carry out the schedule of temperature and pressure over time in accordance with the cure cycle recipe. A typical cure cycle recipe (see Figure 2.1) is comprised of a sequence of segments with temperature and pressure setpoints, and the heating and pressure rates for attaining them. Temperature and pressure transducers monitor the part conditions and provide the feedback signals for closed-loop process control. The recipe requires that each temperature and pressure setpoint is achieved before allowing the process to move on to the next segment.

Often more development work may be required to arrive at a successful cure process that is tolerant of variability of the uncured materials, curing equipment, and tooling. Prepreg materials often exhibit significant batch-to-batch variability and frequently advance with time. To compensate, the conventional approach "builds-in" additional tolerance in the parameter values for this variability in order to yield an acceptable, repeatable, and reliable process. For the cure cycle developer, the initial focus is developing a reliable cure process that satisfies the cure, porosity, FVF, and dimensional requirements. Optimizing the cure cycle is often not pursued once a satisfactory solution has been found.

Physics-based models are often used to simulate some aspect of the outcome for candidate cure cycles in coordination with the experimental work. The following paragraphs discuss useful models for estimating cure, viscosity, and consolidation.

2.4 Temperature and Resin Cure Reactions

The essence of composite processing is the curing reaction of the resin within the prepreg material. Empirical mathematical models that describe the heat of reaction in relation to applied heat over time are widely established. One of the seminal research papers was published in 1982 by Lee, Loos, and Springer (Lee, 1982) for modeling the curing kinetics of Hercules 3501-6 resin. The ability to model the resin cure behavior is the foundation upon which other useful models can be built that are dependent on resin state.

Differential scanning calorimetery (DSC) is a commonly used method for measuring the heat of reaction of a sample in response to temperature changes over time. Both isothermal and temperature ramp conditions are used to portray cure kinetic behaviors. The relation between the reaction rate, $d\alpha/dt$, and the degree of cure, α, where $0 \le \alpha \le 1$ is given by

$$\alpha = \int \frac{d\alpha}{dt} dt \ .$$

An Arrhenius functional form (for instance, Adams and Goldfarb (Adams, 1982)) can be used to estimate reaction rate, after fitting the DSC data to the model. This form of reaction rate model, the "the nth order model", is given by:

$$\frac{d\alpha}{dt} = Ae^{-E_a/RT}(1-\alpha)^n$$

where A, Ea/R and n are material constants.

Another form, the autocatalytic form, which includes an additional term and constant m, is given by:

$$\frac{d\alpha}{dt} = Ae^{-E_a/RT}(1-\alpha)^n(\alpha)^m \ .$$

Artificial neural networks have also been used to estimate reaction rate, as for example by Lee and Rice (Lee, 1997). A neural net is "trained" by learning the input-output relationships based on large amounts of known data. During training, the network adjusts its weights or coefficients that link each neuron in the network, so that the output is correctly predicted from the inputs. Backward propagation is a technique where errors in the input-output mapping are fed backwards, from output to inputs, to correct the weights. The neural network model of Lee et al predicts the reaction rate given the temperature and degree-of-cure inputs.

Other researchers have developed other useful model forms. Ng (Ng, 1999) developed a 3rd order model that worked well with isothermal 8552 data. Shin et al (Shin, 2000) presented a new technique for applying to an autocatalytic model that more accurately predicts the final degree of cure. Costa et al (Costa, 2005) characterized carbon/epoxy 8552 using DSC and rheometer data, as well as dynamic mechanical analysis (DMA) to develop cure kinetics (nth order) and viscosity models

In order to apply a cure model to an actual laminate, the material properties that affect the heat distribution must be accounted for. A commonly used formulation for estimating cure within a laminate is based on the "thermal-chemical" model first proposed by Loos and Springer (Loos, 1983). This model computes the temperature by laminate thickness position as a function of time. The Loos-Springer model is based on the solution of a one-dimensional heat conduction problem with internal heat generation. The governing partial differential equation is:

$$\frac{\partial T}{\partial t} = \frac{K}{\rho C}\frac{\partial^2 T}{\partial x^2} + \frac{1}{C} H_u \frac{d\alpha}{dt}$$

where T is the temperature, t is the time, x is the through the thickness position, ρ is the density, C is the specific heat, K is the thermal conductivity, and Hu($d\alpha/dt$) is the rate of heat generated by the curing reaction. The boundary conditions are the upper and lower laminate surface temperatures which vary with time. The initial conditions are the temperature distribution, $T_o(x)$, and degree-of-cure, $\alpha_o(x)$, inside the laminate at the start of the process. The partial differential

equation above can be solved by writing it in a finite difference form and solving it recursively for every through-the-laminate thickness position.

2.5 Resin State and Viscosity Changes

As the resin is heated during cure, its viscosity first declines to a minimum value and then increases as crosslinking and gelation occur. A rheometer is a standard laboratory instrument used for measuring the change in viscosity that accompanies temperature changes. Rheometric dynamic spectroscopy (RDS) is a widely used method for analyzing the viscoelastic components of the changing resin behavior, as described by R. May (May, 1996). These components include: G', the storage (elastic) modulus, G'', the loss (viscous) modulus, or the complex viscosity ν, a function of G' and G''. Once the temperature and degree of cure are known, some parameter indicative of the resin state and its ability to flow can be estimated. A useful Arrhenius expression for indicating this resin state change is that provided by Ciriscioli and Springer (Ciriscioli, 1990):

$$V = V_m e^{(E_v / RT + k\alpha)}$$

where V is the viscosity and V_m, Ev/R, and k are material constants.

2.6 Pressure and Laminate Consolidation

Consolidation occurs in the cure process by timely pressure application, transverse to the composite plane, to densify the laminate and eliminate non-functional inclusions. Successful consolidation can be described by the proper balance of resin content and fiber volume fraction (FVF) within the laminate, with a minimum of fiber waviness, porosity or voids. Control of pressure is scheduled in accordance with the resin's viscosity so that efficient consolidation occurs without distorting the laminate layers established during layup. A minimum amount of pressure is necessary to ensure low porosity and negligible voids are achieved. Since the pressure also forces the laminate against its tooling surfaces, it establishes the final cured part shape and dimensions.

The timing, duration, rate, and the magnitude of pressure application are crucial. Pressure duration and magnitude can cause excessive resin flow, resulting resin-starvation within the laminate. Resin starvation adversely impacts the composite strength, since this condition exceeds the acceptable fiber volume fraction range. Similarly, pressure application too soon in the process can entrap volatiles in the material.

2.6.1 Consolidation models

Consolidation behaviors have been studied by several researchers, including Dave, Kardos, and Gutowski. The most established and largely equivalent models are those of Dave and Gutowski. Research by Gutowski et al (Gutowski, 1987) investigated the relation of applied pressure and pressure within the resin during consolidation. He found that initially all applied pressure was reflected in the resin pressure, but as consolidation proceeds, the fiber volume fraction increases. The fibers within the laminate form a network that elastically deforms under the increasing load. But increasingly the applied pressure is split disproportionately to the fiber bed, so much so that it is possible that the resin pressure can actually be lower than the applied pressure. This is of major concern since adequate resin pressure must be maintained so that porosity and voids are suppressed.

Permeability of the fiber bed is a key variable affecting resin flow for press molding. As the laminate is consolidated, permeability decreases, hindering resin flow. The resin transfer molding process consists of the introduction of pressurized resin into a preformed fiber structure. Rodriguez et al (Rodriguez, 2004) investigated the permeability–porosity relationship in an RTM process for both glass and natural fiber mats.

2.7 Improved Approaches To Cure Process Optimization

Researchers have developed systems that employ rule-based heuristics and strategies to improve on trial and error approaches to develop successful cure processes. These strategies are based on signposts or hallmarks of distinguishable states that occur through the course of the process. Once these signs are detected, then appropriate actions can be taken to

keep the cure on track. Examples of these rule-based systems are Qualitative Process Automation for Autoclave Curing of Composites (QPA), Abrams et al (Abrams, 1983) and SECURE, Cirisioli and Springer (Ciriscioli, 1990). QPA translates sensor information into a qualitative cure state description (e.g., resin at minimum viscosity) by a "parser" which is analyzed by an expert system. The expert system in turn makes and executes control decisions to the autoclave to attain desired material properties. SECURE is similar to QPA in that it interfaces expert system rules and sensor inputs while generating the required controller outputs. These systems represent improvement over trial and error methods by imposing some structure and discipline to what had previously been largely a “black art”. They also produced more consistent yields and reduced cure cycle times. A limitation of such expert systems is that they are very domain-specific in regards to the material system and process being used, as opposed to being more general in nature.

Artificial neural networks (ANNs) have also been used by many researchers to capture or “learn” a complex nonlinear relationship between input-output data. After the ANN has been taught, it can be a very efficient representation of this mapping, and then could be employed within a control system or optimization scheme to efficiently emulate the complex system it was patterned after. Nielsen (Nielsen, 2002a) used a neural net to estimate the changing in-process permeability of a fiber preform in a series combination with other model types to construct a control system for resin transfer molding. ANNs are useful where abundant data exists for its structured training, where input-output relationships are relatively static, and where there is no interest in knowing or understanding the driving variables and the nature of their relationships to outputs. However, ANNs have major shortcomings to deal with, such as learning and overlearning, and how to incorporate new data. Another is the lack of transparency in the input-output relationships that could provide useful insights into the nature of the problem domain. Nielsen (Nielsen, 2001) applied physics-based process simulations to the training of an artificial neural network (ANN). The ANN was then used for real-time process simulations, where a

simulated annealing algorithm was used to derive the optimal real-time control decisions. A key variable was estimation of in-situ preform permeability in real-time. Other researchers have applied ANN models to experimental data, such as Ciurana et al (2009).

Traditional methods of optimization are gradient (derivative)-based. Regression models (such as described by Kutner, 2005) are well established in linear and nonlinear forms, and well suited for predicting the value of a single response variable in terms of independent variables or factors. Response surface methodology (RSM) is probably best suited for a complex multivariable situation, or where the exact nature of the functions is not known, or well understood, as exemplified by Sheldon et al (Sheldon, 2001). Other researchers have applied RSM to summarize input-output datasets generated by Monte Carlo simulations over ranges of values for each input parameter to explore an n-dimensional space. Both regression and RSM models can be developed based on sufficient experimental data.

Numerical based approaches to optimization, however, require knowledge of governing equations, transfer functions, and so on. For a process that is complex, has many factors suspected of being related to the response variable(s), and is not well understood, a conventional approach for investigation is to use designed experiments. The most commonly applied are a factorial or Taguchi experiment that is designed and carried out, featuring multiple factors and levels, to explore the relationships to the critical outcomes, desired responses or quality variables. Often analysis of variance (ANOVA) techniques are used to determine the major or significant factors, most correlated to the responses. Experimental data may then be fitted to regression or response surface models, with confirmation process runs used to validate model predictions. Optimization can then be explored via the models. Examples include Palanikumar (2008), Walia et al (2006) and Yang (2006).

State of the art cure process models typically utilize finite element models (FEMs) to capture the full extent of its complexity. These models are widely used to provide high fidelity physical models for process development and improvement studies, as by, for example, Chen

(Chen, 2002). However, because they tend to be granular in their detail, FEMs require specialized knowledge and expertise to fully exploit. These models may also be difficult to integrate within an optimization scheme, so that their application to cure process optimization often proceeds along a path of trial and error. In contrast, finite difference models (as described by authors such as Chapra, 2006) can deliver a acceptably high degree of fidelity and accuracy, are computationally efficient and more readily suitable to be applied in control system and optimization algorithms. The Adaptive Control Cure Monitoring (ACCM) system (Saunders et al, 1999) is an example of a computer control system incorporating on-line finite difference models to provide real-time estimated data to augment sensor-based data.

Finite difference-based model building blocks have also been integrated within a comprehensive simulation modeling system, utilizing gradient-based approaches to seek an optimal cure cycle. Rai and Pitchumani (Rai, 1997), employed such a modeling approach in developing a systematic methodology to finding the optimal temperature and pressure combination for autoclave laminates. A sequential quadratic programming (SQP) method was utilized to determine the shortest cycle completion time, subject to process constraints. They generalized the cure cycle as represented by a series of piecewise linear segments for both temperature and pressure. The temperature cycle was made up of endpoint temperatures for each segment and the respective segment time durations. Similarly the pressure cycle was made up of segment pressure levels extending over segment durations. The optimization algorithm utilized the SQP nonlinear optimizer with the numerical process simulator, along with a decision block to evaluate the satisfaction of the optimality conditions. The optimizer invoked the numerical model with values for the 8 temperature decision variables, the 4 segment temperatures and durations. The numerical model then returned values of the cure time with values of the constraint equations. The optimizer calculated the partial derivatives by perturbing the values of the design/decision variables and observing the corresponding changes in the objective function and the constraints. The cure pressure cycle optimization subproblem was

solved in a similar manner, using the values obtained from the optimal cure temperature cycle. The iterative sequence through the optimizer and numerical model and decision block was carried out until the optimality conditions were satisfied. At convergence, the values of the decision variables constituted the time-optimal cure cycle. Nielsen (Nielsen, 2002b) used finite difference numerical models to simulate a resin transfer molding (RTM) process. The simulation was used on-the-fly in real time to predict and guide controller decisions. The controller accomplished uniform mold fill by controlling the flow rate of three independent resin injection pumps.

Citing limitations of gradient-based methods, many researchers have employed evolutionary methods such as genetic algorithms (GAs) As pointed out by Bag et al (2009) classical gradient-based search techniques may not be optimal in the sense that they can be trapped in local minima and require the objective function to be continuous within the search space. In contrast, stochastic optimization techniques, such as GAs, can overcome these difficulties and are capable of finding the global solution. Other evolutionary methods include simulated annealing and differential evolution. Pettersson et al (2009) used a GA yielding states of operation for a blast furnace on a Pareto-optimal front with nondominated solutions. Mitra et al (2009) carried out multiobjective pareto optimization for an iron ore induration process using an evolutionary (GA) algorithm. Mahfouf et al (2005) used GAs to tackle optimization of heat treatment and chemical constituent percentages for steel alloys.

2.8 Material And Process Variability Effects On Optimal Cure Cycles

The types of empirical cure and viscosity models previously discussed provide good predictions in relation to the actual measured data that are based upon. These models are routinely used as if they are deterministic in nature, but this does not account for several sources of variability seen in practice. Composite materials can exhibit significant batch -to-batch variability and undergo out-time effects that can significantly change their behaviors

during cure and consolidation. In addition, most models use regression techniques of least squares to fit the parameters to the data.

As explored by Padmanabhan (Padmanabhan, 1999), the sensitivity of the model parameters and the lack of fit of the model to the underlying data translates into sizable differences in predicted resin reactivity and its state of advancement. Stochastic Monte Carlo methods were used to investigate the range of effects on cure time. The effects on model predictions of various amounts of normalized standard deviations were simulated with respect to the deterministic Arrhenius cure model parameter value (the mean). This research underscores the overall impact to model estimates of small differences in parameter values, most often taken as constants.

Utilizing a range of values for model parameters may better represent the variability in the material properties and constituents. Thus, if these parameters follow a normal distribution, then the expected value of the consequences of any given cure cycle will also follow some distribution. Therefore the optimal cure cycle will vary depending on these distributions. This concept was discussed by Mawardi (Mawardi, 2004). A stochastic model was developed using uncertainties defined via probability distributions. The model was then applied to a deterministic process, conducted by way of numerical simulations, to quantify the output parameter variability. A variant of Simplex method and simulated annealing were used with the stochastic model to determine the optimal cure cycles. A critical level of uncertainty in model parameters was identified take into account when applying to a deterministic “optimal” cure cycle.

2.9 Conclusions and Dissertation Approach

Thick structural aerospace / rotorcraft composite parts are highly loaded and are flight-safety critical components. They are also very challenging in their manufacture. A representative, generic part configuration for such a part is a flexbeam, thickest on one end, not as thick on the other end, and tapered down to its thinnest dimension at mid-length.

A successful cure process must be efficient in time and cost, while satisfying its minimum requirements. Controlling this process is essentially managing the interactions of temperature distribution, degree of cure, laminate thickness, and void content by manipulating only the press temperature and pressure. Design of a cure cycle that consists of temperature profiles along with adequate pressure over time can ensure an acceptable cure. Models built on the Loos, Springer (Loos, 1983) thermochemical model foundation are well established in the literature and are widely used in process development. In attempts to optimize the overall cure process time, Rai (Rai, 1997) was able to apply numerical physics-based model to seek optimal cure cycles assuming a standard fixed rate pressure application in an autoclave.

While numerical based optimization approaches are well suited to focus on the objective function of minimum overall cure time, there are other considerations that knowledge-based approaches contribute that are important for part quality and uniformity. For example, it is critical that the laminate be uniform in resin state prior to pressure application so that as uniform as possible resin flow and fiber volume distributions result before completion of resin cure. The approach to optimizing the cure cycles for the thick laminate flexbeams in this study combined the benefits of rule-based methods with numerical optimization.

Fiber waviness (as discussed previously) is a major manufacturing defect issue that compromises structural strength and part longevity. Some research has investigated the causes and remedies for this defect, with some experimental results for what process parameters seem to work vs. not. However, there has been a lack of a explicit or formal description, definition, or explanation of the underlying mechanisms. An explanation that will be pursued here is this: the nature of a flexbeam laminate being cured in a closed-cavity mold is that consolidation during cure reduces the laminate thickness disproportionately with respect to its uncured thickness. Since the mold is designed to yield the final desired laminate thickness dimensions, there will be a mismatch of inner mold surface dimensions with the uncured laminate dimensions, creating areas of noncontact (gaps) towards the middle of the flexbeam length. These gaps will exist

initially in the cure process but will be closed later during consolidation. For a flexbeam within a closed cavity tool, applied pressure to consolidate the laminate is applied generally normal to the lengths of the plies. Applied pressure will generally be directed downwards to collapse spacing between plies, increasing resin pressure, and forcing resin to flow out. However, resin flow is suspected of imposing an axial force that would lead to/ cause fiber buckling, leading to waviness. Fiber waviness would be considered hard to form if a sufficiently large normal force was always imposed during consolidation, since it would keep all plies length-wise parallel and "flat". The velocity of this resin flow is suspected to be a function of the applied pressure (along with resin properties, flow impedance, etc.). In order to reach desired consolidation there can be different pressure application schedules, some of which that could produce high resin velocity. Because a flexbeam is predominantly comprised on plies running lengthwise, with accompanying predominantly axial permeability, the predominant resin flow will also be axial, or length-wise for the part. If the resin velocity running through the plies in a local region is excessively high, relative to the normal force imposed over those plies, then fiber waviness could occur. This dissertation will investigate how to minimize the overall cure process for a flexbeam thick laminate with focus on the consequences of consolidation.

The objectives of the model to be utilized is presented in Chapter 3. Chapter 4 presents the optimization of the cure process of a thick flexbeam composite laminate. The model output was analyzed to investigate the origins of fiber waviness and the effect of material thickness variation. Two representative materials were utilized for the flexbeam laminate to compare/contrast their optimized processes.

CHAPTER 3

THE CONSOLIDATION-RESIN FLOW MODEL

3.1 The Cure Process Model

The basis for optimization of a cure process was selected to be a representative rotorcraft thick composite part with its associated closed-cavity tooling for curing in a bond press. A flexbeam was selected as a representative composite laminate, to be modeled utilizing two representative material systems, IM7/3501-6 graphite/epoxy and S2/8552 glass/epoxy. A generic flexbeam was designed, 6 feet long and 2” thick at one end and 1” thick at the other end, with its closed-cavity press tooling.

The original plan was to run iterations of a commercial finite element model (FEM) of the flexbeam as the basis for cure process optimization. The data for the generic flexbeam and its closed cavity press tooling were input into the software to create a 3-dimensional model. Figure 3.1 displays the FEM of the generic flexbeam with its tooling. Notice that the laminate is enclosed within the tool cavity, with the matching tool lid on top. The lid has an inside surface that directly contacts the laminate and constrains its dimensions and contours. The model was comprised of a pressure-driven consolidation submodel, and a thermally-determined cure and viscosity submodel. The soil material element of the of the FEM software, a porous media having solid and fluid components, was to be used to simulate the consolidation of the laminate due to pressure application. This approach has been used with some success in modeling a composite part, since it also consists of fluid (the resin) and solid (the fibers). When the soil material is consolidated, changes occur in the 3 variables that characterize consolidation: laminate volume is reduced through displacement changes to increase density, porosity is reduced, and pore pressure increases. Displacement refers to changes in the height of the

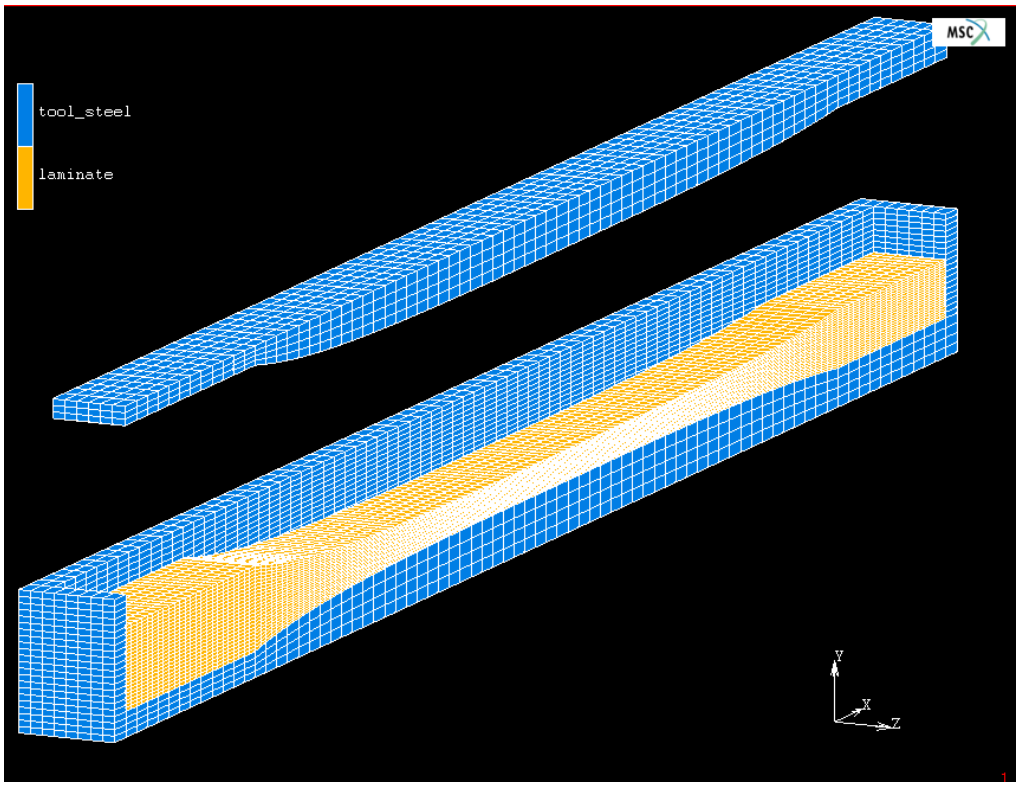

Figure 3.1. Generic Flexbeam with Tooling Model.

laminate volume. Porosity measures the proportion of total volume that is open space (no fluid or solid). Pore pressure represents the fluid pressure within the soil mixture of solid and fluid. A separate FEM model having the same flexbeam geometry was developed for modeling the cure process thermal behaviors, using thermal elements. These were aimed at predicting temperature changes due to tool contact during the cure process as well as the heat of reaction. The 3D FB model was very granular (about 21,000 elements) and produced problems in running and running efficiently for iterations; the results for many runs of the model were not reliable.

In addition to difficulty in running the model, the most crucial finding with the use of this FEM software was that is not capable of realistically simulating the entire cure process. It could not support a fully integrated (or coupled) model consisting of the resin pressure and

consolidation submodel with the thermal cure and viscosity submodels. The principal shortcomings were the following:

(1) The effects of resin viscosity changes on the resin pressure and flow within the consolidation submodel were not linked to the thermal degree of cure and viscosity changes.

(2) The soil-based resin flow and consolidation submodel splits the applied pressure between the solid and fluid components of the soil, determined by the user-specified elastic modulus value for the soil solid component. The remaining pressure is applied to the resin/pore pressure. Consolidation increases in porosity (soil) or fiber volume fraction (composite) were not accompanied by the required nonlinear increase in stiffness that characterizes composites.

(3) Consolidation changes to fiber volume fraction were not coupled to changes that would occur in permeability of the laminate material.

(4) The software was not very open, accessible, or transparent so as to allow the user to customize the model for specific objectives.

A simplified FEM composite model was developed and exercised to explore the behaviors of pressure application and consolidation. It was constructed of a simple cube (1 m x 1 m by height 1 m) of soil material onto which was applied a rigid surface to simulate the tool lid imposing pressure downward onto it. The purpose of the simplified model was to investigate pressure application and its effects on displacement, porosity, and pore pressure for application to a new model. It was expected that the reduced laminate volume would occur equally with respect all directions, resulting in a uniform increase in laminate density. The model set-up was to apply pressure on the top surface to reduce the volume of the laminate, while constraining the sides and bottom from moving or expanding, to simulate tooling constraints. A pressure film coefficient was assigned to all nodes on the 4 vertical sides to simulate resin flowing out. The pressure film was used to reduce pressure incrementally, analogous to Newton's law of cooling:

Resin pressure$_{t+1}$ = resin pressure$_t$ (1- hp) where h_p = film coefficient and $h_p < 1.0$

Permeability describes the resistance of a porous media to the flow of a wetting fluid. Different permeability values were defined for the x and y orientation of the laminate material: the x permeability was set larger to simulate longitudinal vs. transverse permeability. Each strata (arrangement of nodes running across) of the laminate were consolidated (z-wise) uniformly, and the reduction in volume was also uniform with respect to the z direction. Displacement z values were linearly and proportionally divided from the top to bottom nodes of the body. This even distribution indicated that compaction or change in volume for any layer in the laminate is the same. This was verified from the porosity values being the same for all nodes with respect to time.

The pore pressure values were found to be identical at each z level for each vertically aligned node. This indicated the effect of the applied pressure on the top layer of the laminate is equally felt at all layers from top to bottom. Likewise, the film coefficient permeability of all external side nodes was identical, so the nodal pore pressure distribution moving x or y-wise from the center to the edges (where pore pressure was set to zero) was found to be a function of the fluid flow through the x and y directional paths. This was in turn dependent on the x and y directional permeability properties of the soil material. Each of these “flows” wais much different, even though the resistance of the face pressure film coefficient was the same value. The flow pattern followed a parallel electrical circuit where each flow x-wise and y-wise originate from the center and proceed to the edges independently, but subject to different flow restrictions.

3.2 Objectives for The New Cure Process Model

Because of the difficulties with the FEM, a new model was built from scratch. Its major goals were:

(1) A simple but sufficiently adequate and comprehensive composite laminate model to characterize the major changes that occur in the cure process for a closed cavity press environment and used for optimization studies.

(2) An integrated and coupled capability for the pressure-consolidation behaviors with the thermal-cure behaviors, based on resin viscosity changes as a result of cure.

(3) Thermal modeling to include heat of resin cure reaction as well as heat from press tooling/lid, dependent on surface contact.

(4) The capability and flexibility to adapt and expand the model to investigate specific process scenarios.

3.3 New Model Approach and Assumptions/Groundrules

Certain simplifying assumptions were made while building the model. A flexbeam type part was chosen because it is relatively simple in geometry, is often cured in a press, and because of its thickness, can pose significant cure control challenges. Because the geometry of a flexbeam is planar, that is, it has height that differs over its length but not over its width (or depth), the 2D model was deemed to be adequate to characterize the part. The predominant prepreg material fiber orientation used for the flexbeam is along its length (0 degrees) for tensile strength. The longitudinal permeability that is associated with this orientation is 2 to 3 orders of magnitude higher than the transverse permeability. Thus, the model was built with the philosophy that the predominant resin flow for a flexbeam is in the x direction, i.e., along its length.

The model does not include mass properties of the resin or fiber in the flow and compaction behaviors. Mass properties are assumed to include momentum, inertia, and time-dependent effects of resin from viscous flow. The goal of the model is to find, investigate, and detect worst case conditions in simulated real-time. Mass properties were deemed less critical to include during the critical part of the cure process when temperature is being applied up to its final temperature and pressure is being applied up to its final level. During this phase, most defects occur. The focus of the model was on resin pressure and flow patterns. During this phase of the cure cycle the applied pressure is generally monotonically increasing. At certain points, there are applied pressure dwells, during which the resin pressure is expected to bleed off, and could cause some porosity if not followed soon with resumption of higher applied pressure. This model was designed to be simple and straightforward but comprehensive in areas that are suspected to shed the most useful light on suspected areas. The resin flow

patterns velocity and timing during the process are the major suspects for causing fiber waviness or marceling. The inclusion of thermal effects of temperature and cure on the viscosity of the resin via Darcy's law are known factors affecting velocity. The model was intended to indicate optimal vs. problematic cure process parameters or scenarios that could create defects. These scenarios could then be investigated by work on actual laminates.

3.4 Introduction to the Pressure and Consolidation Submodel

A critical portion of the cure process model characterizes the consolidation of the composite laminate as pressure is being applied during the cure cycle. The application of pressure to the laminate brings about displacement and volume changes with resin flow out of the laminate. Laminate volume is occupied by fiber, resin, and to a much lesser degree, by air that is entrapped during layup, or volatiles as a by-product of curing. The process of consolidation during the application of heat and pressure of the cure process forces resin flow out, while reducing the spacing between the fibers, forming a more dense mixture. Void volume is defined as the relative volume not occupied by fibers or resin; therefore, it is a defect within a cured laminate. A principal objective of curing is to apply adequate pressure to minimize porosity. The flow of resin is also an aid in "wicking out " entrapped air or gases out of the laminate. For the 2 materials being utilized for this research, IM7/3501-6 and S2/8552, the fiber volume fraction for a consolidated laminate typically ranges between 50 and 65 percent.

3.5 Darcy's Law

The laminate being modeled contains both resin and fiber volume and is considered to have negligible void volume. The focus of the pressure submodel is on the distribution of resin pressure within the laminate and its resulting resin flow due to pressure application. For a press cured part, pressure is applied through contact with the tool lid surface as depicted in Figure 3.2. For a simple flat laminate, if pressure is applied uniformly across the top surface, then the resin pressure within the laminate will increase, causing resin to flow to its outside edges. Here the resin pressure at the edges of the laminate is assumed to be zero, and pressure is at its

maximum at x=0. Resin flow will then occur as a result of the differential pressure, moving from the higher resin pressure to lower. The result will be a reduced laminate resin volume, a

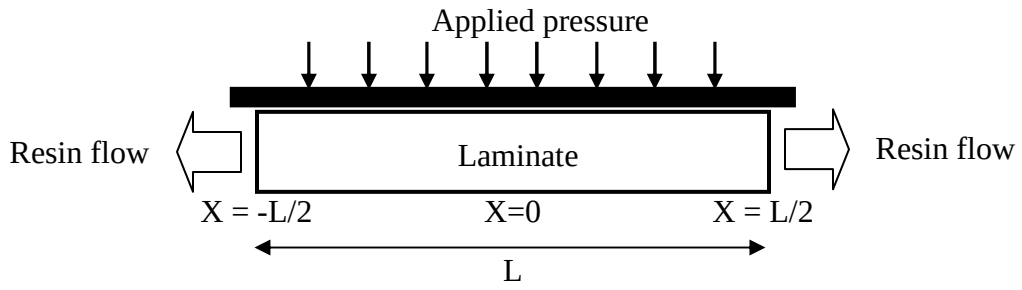

Figure 3.2. Consolidation of a Flat Laminate with Pressure Applied by a Rigid Surface.

displacement change for the top surface and a reduced overall laminate volume. Here it is assumed that the predominant fiber orientation for the laminate is along its length; therefore in reference to the figure, the predominant resin flows will be horizontal, flowing out the edges on either side.

The velocity of a fluid through a porous media of unit cross-sectional area is governed by Darcy's Law:

$$\text{Resin flow velocity} = \frac{K}{\mu}\frac{dP_r}{L}$$

where the differential resin pressure dP_r (Pa) exists between 2 points separated by a distance L (m), K is the permeability (m^2), and μ is fluid viscosity (Pa-sec). For application to flow through a composite laminate, all laminate volume is assumed to consist of fibers fully saturated with resin, with negligible void volume. Note that permeability can be thought of as a proportionality constant that accounts for the pressure drop through the laminate under conditions of a constant flow rate.

3.6 Permeability

Permeability is a fundamental material property for resin flow characteristics through a laminate. Gutowski proposed an expression for permeability based on the Carman-Kozeny constant k_{ii}:

$$S_{ii} = \frac{r_f^{\,2}}{4k_{ii}} \frac{(1-V_f)^3}{V_f}$$

where r_f is the fiber diameter (m) and V_f is the fiber volume fraction. Figure 3.3 portrays the permeability as a function of V_f.

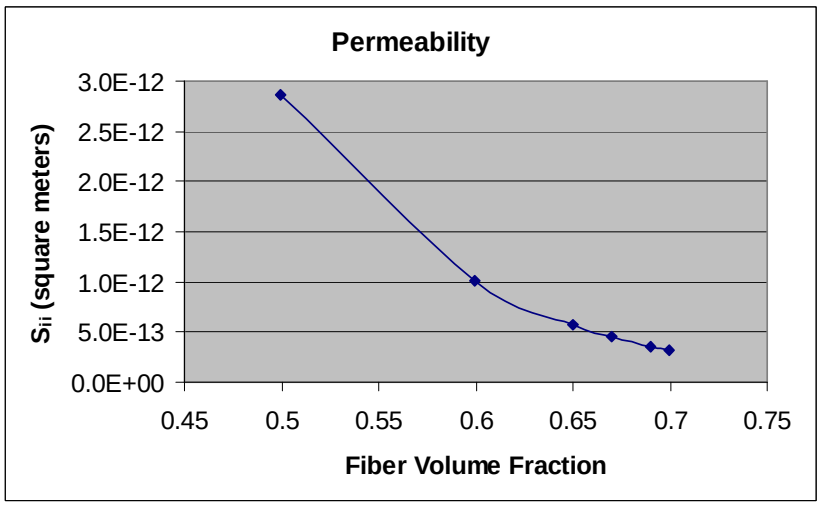

Figure 3.3. Permeability as a Function of Fiber Volume Fraction.

Gebart [1992] also proposed expressions for both longitudinal and transverse permeability which have been adopted in the model. The principal permeability directions are longitudinal (along the fiber direction) as given by

$$K_l = \frac{8r_f^{\,2}(1-V_f)^3}{gV_f}$$

and transverse (90° to fiber direction), as is sim ilarly given by

$$K_t = C\left(\sqrt{\frac{V_{f\max}}{V_f}} - 1\right)^{5/2} r_f^{\,2}$$

where V_f is the fiber volume fraction, r_f is the fiber diameter (m), and g is a constant. Values used are r_f = 5μm for IM7 fibers, V_{fmax}=0.785, C= 0.4, and g= 57.

3.7 Viscosity

Viscosity is the property of a fluid to flow when pressure is applied. Numerous resin viscosity models have been proposed, including that by Ciriscioli and Springer. The model will utilize the Ciriscioli viscosity model for both composite materials used in this research:

$$V = V_m e^{(E_v / RT + KV\alpha)}$$

where V is viscosity in Pa-secs, and V_m, Ev/RT, and KV are material constants.

3.8 Gutowski Effective Stress and Resin Pressure

Gutowski [1986,1997] explored the relationship between the applied pressure and the resin pressure during consolidation of a laminate. The applied pressure was found to be shared between a stress that compacts the fibers and the resin pressure. The aggregate of all the fibers constitute a fiber bed, able to carry a substantial load as the fibers are increasingly packed together. At any time the total through the thickness stress σ is shared by the fiber bed and the resin, maintaining the following equilibrium equation:

$$\sigma = \bar{\sigma} + P$$

where $\bar{\sigma}$ is the effective stress in the fiber bed and P is the resin pressure. The effective stress is given by

$$\bar{\sigma} = As \frac{(\frac{V_f}{V_0} - 1)}{(\frac{1}{V_f} - \frac{1}{V_a})^4}$$

where As is the fiber stiffness, V_f is the current fiber volume fraction, V_0 is the fiber volume fraction at t=0, and V_a is the maximum allowable fiber volume fraction. The effective stress applied to the fiber bed is a function of the fiber volume fraction V_f, thus the ability of the fiber bed to sustain a load increases like an increasingly stiff spring. When pressure is applied initially, V_f is at the low end of its range, and all applied pressure is applied to the resin. As consolidation continues, the resin pressure and resulting flow increase the V_f so an increasing

proportion of the applied pressure is applied to the fiber bed. As V_f approaches its maximum value, all applied pressure is applied to the fiber bed, and the resin pressure can deteriorate. Figure 3.4 presents the relationship between the effective stress ESS and V_f for a fiber bed of AS4 fibers.

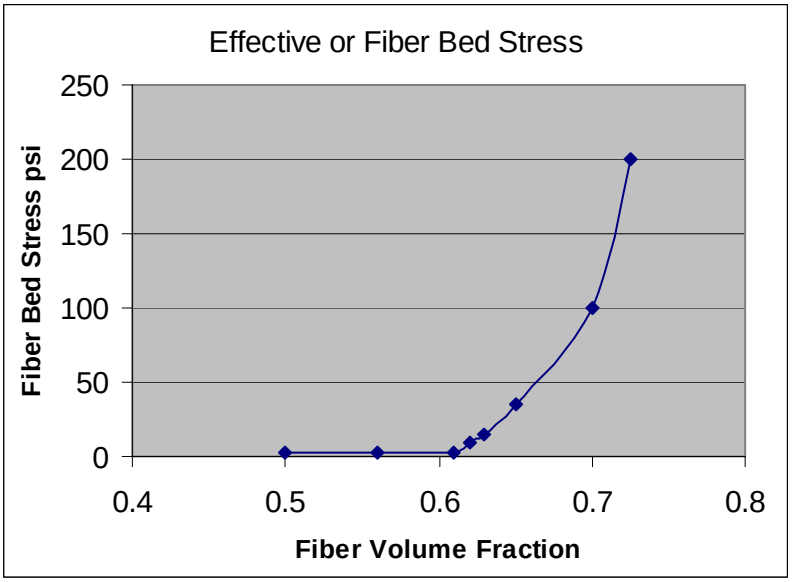

Figure 3.4. Effective or Fiber Bed Stress vs. Fiber Volume Fraction.

3.9 Hubert Fiber Bed Compaction Curve Experiments

The fiber bed compaction curve defines the relationship between the effective stress and fiber bed deformation. Hubert (Hubert, 1996) conducted experiments that explored the essence of laminate consolidation and demonstrated a method for determining the fiber bed compaction curve. Special load apparatus and tooling were used to apply a clamping load to a flat laminate while constraining its motion but allowing resin flow to exit from its sides. The laminate was comprised of 16 plies of AS4/3501-6 (fiber/resin) and was compacted in a series of constant displacement rate ramps followed by a displacement hold condition. For each displacement step, a clamping pressure ramp was controlled to produce a uniform displacement rate. As each displacement position was held, the required load necessary to maintain this position was monitored and found to relax as the resin flowed out. When the required load

reached a steady state, this value was taken as the effective stress for the laminate at that displacement position. Each displacement step value and its corresponding required effective stress was recorded. The final fiber bed compaction curve was calibrated by using an independent laminate consolidation sample under a constant applied pressure to achieve full consolidation.

3.10 The Flat Laminate Model

A simple 2+1/2 D model of laminate consolidation and resin flow was developed to emulate Hubert's (Hubert, 1996) experiments. The model represents a flat laminate (length x, depth y, height (h) z) and is based on a single volume that is a homogeneous mix of 3501-6 resin and AS4 fiber. A major objective of the model was to demonstrate how the resin pressure deteriorates during a displacement dwell condition. The model was designed to simulate 3 modes of load conditions and determine the appropriate applied pressure for each simulated timestep:

- Mode 1: Apply pressure ramp to achieve desired displacement z rate per delta time
- Mode 2: Hold pressure constant and allow resin pressure to bleed off (via P film)
- Mode 3: Hold current height z position: maintain pressure = current ESS and allow resin pressure to bleed off

Applying pressure causes resin to flow out, reducing the overall laminate height and volume, and increasing the fiber volume. The resin is assumed to be incompressible; therefore, there is no change in laminate height without resin flow out. Applied pressure (P_{appl}) is assumed to be uniform across the laminate top surface. It is also assumed that any effects or changes to the laminate as a result of compaction are uniformly distributed throughout the laminate volume. At any time the laminate can sustain an effective stress load or effective sustainable stress (ESS) which is dependent upon the current V_f, as described by Gutowski. As resin is squeezed out of the laminate, the V_f increases and so does the ESS capability of the laminate. The permeability is calculated as a function of V_f using Gebart's longitudinal permeability equation.

At any timestep in the simulation, the model maintains the value of the top laminate surface height h, the current resin volume, V_f, and ESS for the current laminate state. At the beginning of the simulation (time =0) the resin occupies one half of total laminate volume. For any subsequent time, the resin volume flow rate from the previous timestep is used to update the current resin volume, the laminate h, and the total laminate volume. From this the new V_f is calculated and then used to update the ESS that the laminate is capable of sustaining. The ESS is then used to determine the new resin pressure. Under conditions of a monotonically increasing applied load, i.e., Pappl at time t >= Pappl at time t-1, these rules apply for each timestep:

1. If P_{appl} < ESS [early on in P application], then there is insufficient pressure to compact. Since P_{appl} =ESS+resin pressure, there is no resin pressure to cause flow.
2. If the P_{appl} > ESS then since P_{appl} =ESS+ resin pressure, compaction occurs and (additional) resin pressure causes resin flow in concert with (additional) compaction movement. As h is lower, the overall laminate volume is reduced. Since the fiber volume remains unchanged, and the resin volume decreases, and V_f increases.
3. If P_{appl} =ESS, then no (further) compaction occurs and the current h is maintained. Since P_{appl} =ESS+ resin pressure, no further addition to resin pressure occurs and resin pressure bleeds off. Whatever resin pressure exists continues to cause resin flow in accordance with Darcy's Law.

For mode 1 operation, the model iterates to find a value of Pappl that will result in a change in resin volume to yield the target displacement change rate from the preceding timestep. The actualESS is calculated from P_{appl} vs. ESS, and is used to determine the resulting resin pressure. If the actualESS is at least as large as ESS, then the remaining pressure from P_{appl} is applied to the resin pressure:

1. If P_{appl} > ESS then actualESS = ESS and resin pressure = P_{appl} – ESS.
2. If however $P_{appl} \leq$ ESS, then actualESS= P_{appl}, and resin pressure is allowed to bleed off, using a pressure film coefficient h_p value set =0.097.

For any timestep the resin pressure is used to calculate the resin flow velocity from Darcy's Law, and the resin flow volume rate based on the current cross-sectional area. At the beginning of the next timestep, the new resin volume is calculated by subtracting the resin flow volume rate * delta time from the previous volume. The last resin pressure level is not maintained or used for the next timestep when P_{appl} is monotonically increasing. Each timestep is then treated discretely with respect to resin pressure: the new P_{appl} value is applied to the split of resin pressure vs. ESS based on V_f. New resin pressure value is not added to the previous one. However, when a constant P_{appl} (mode 2) or a constant Z position (mode 3) is used, a resin bleed mechanism utilizing the pressure film approach is used.

Hubert used an independent laminate sample to achieve full consolidation achieving a final strain point of 0.184 and serve as a reference for calibration of the compaction curve datapoints. The flat laminate model prediction was close to this, achieving strain of 0.202. The following 2 figures illustrate the validation of the flat laminate model in relation to Hubert's work with fiber bed compaction curves. Figure 3.5 displays the total pressure required to produce a

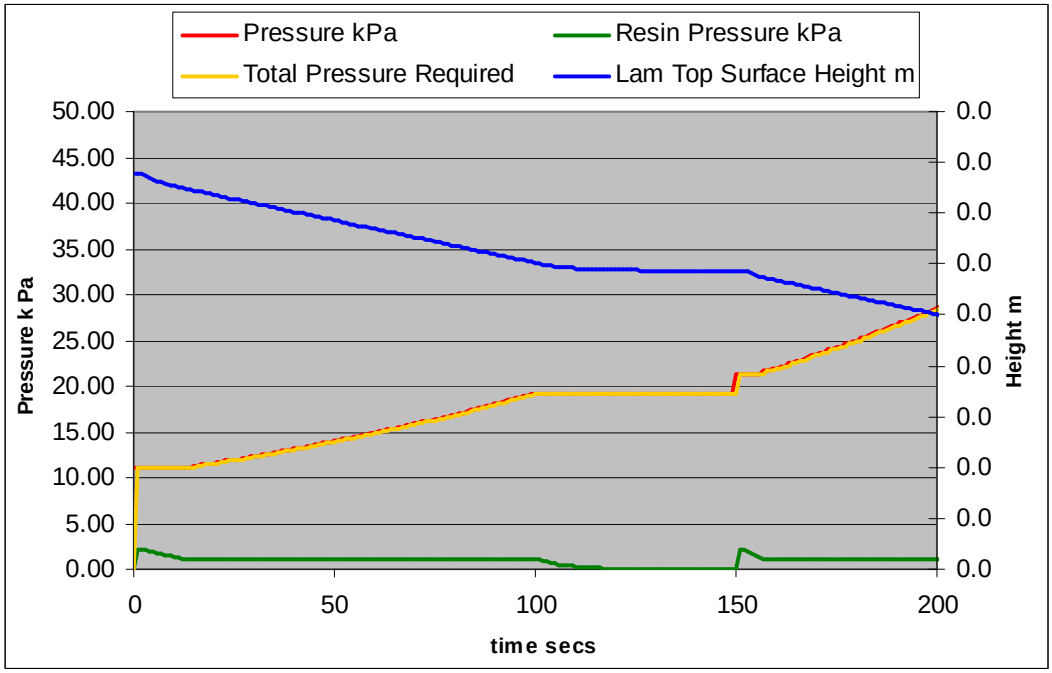

Figure 3.5. Flat Laminate Model Constant Displacement Rate and Position Hold.

constant displacement ramp followed by a dwell at the current laminate top surface height position. The decay of the resin pressure can be observed during the dwell. Figure 3.6 demonstrates a constant pressure dwell (Mode 2) scenario. Note that this model uses a fixed permeability value of 2E-10. A more realistic model includes Gebart's permeability, a function of Vf. Figure 3.7 shows how the final laminate height is arrived at for that model and is held due to insufficient pressure to further consolidate the laminate, based on ESS. This model also achieved a final strain of 0.2018.

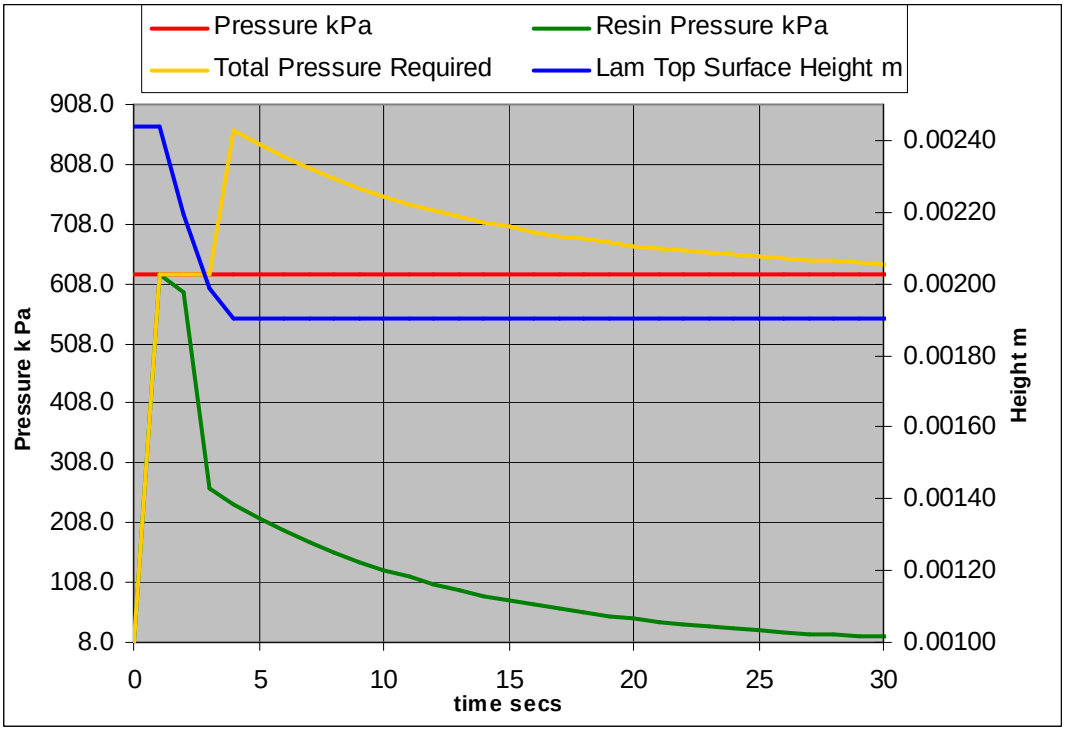

Figure 3.6. Flat Laminate Model Constant Pressure Dwell.

3.11 Concluding Thoughts on the Flat Laminate Model

The variables in Darcy's Law were found to be the fundamental factors affecting the compaction behaviors. As was expected, changes to either permeability or viscosity changed the rate at which compaction occurred and reached a laminate height plateau. The final height was a function of ESS, and when pressure applied became insufficient to overcome this stress,

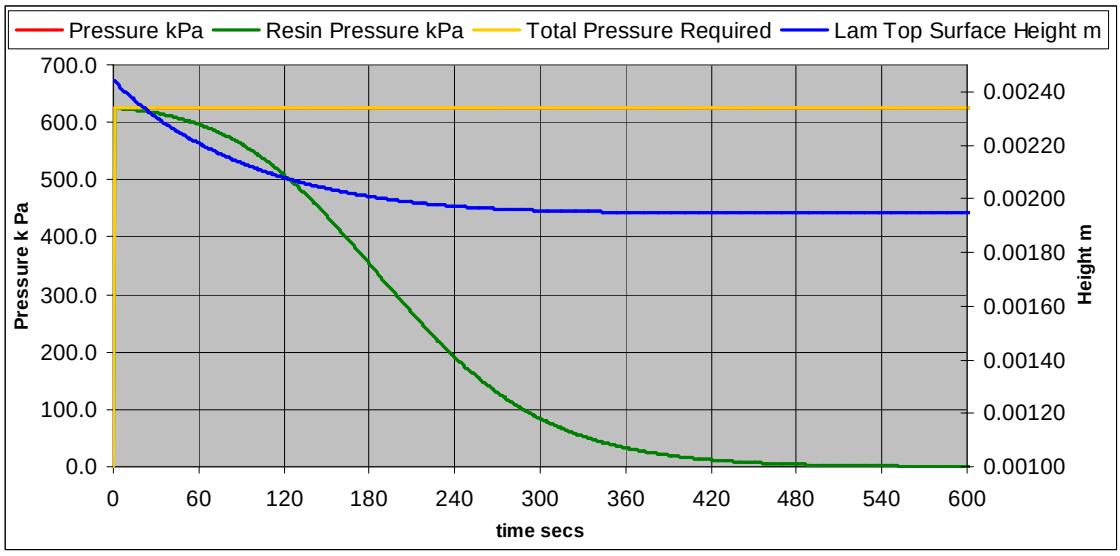

Figure 3.7. Flat Laminate Model Constant Pressure Dwell with Permeability as a Function of V_f.

there was no further compaction movement. Changes in V_f required significant increases in Pappl to continue compaction.

3.12 The Flexbeam Laminate Model Geometry, Control Volumes and Nodes

The laminate is modeled as a 2+1/2 dimensional body having length x and height z dimensions with a constant depth dy. The laminate interior volume is subdivided into n x n control volumes (CVs), and 2n additional CVs for its exterior, each possessing resin volume and fiber volume and assuming negligible void volume. For each position x separated by dx, the laminate top surface height is divided into n CV heights, so the height of a CV differs with differences in the laminate height.

Figure 3.8 portrays the CVs and nodes within a simple flat laminate. The sum of all CVs' resin and fiber volume represents the overall laminate during the cure process. The 2D geometry of a CV is defined to be rectangular (x width, z height, and dy depth). Two nodes are associated with each CV. The top node (blue) monitors its top surface (z) height due to compaction and contact. The other node (yellow) defines its mid-width and mid-height (z) position and is used for determining resin flow velocity and temperature estimating. Interior

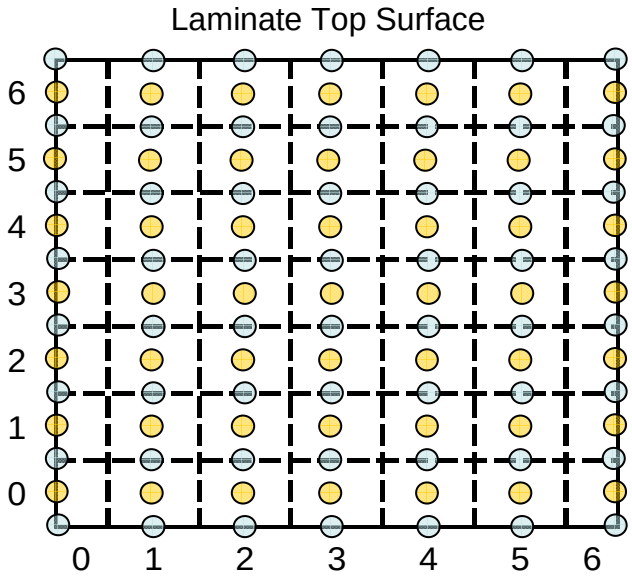

Figure 3.8. Model Control Volumes and Nodes Representing a Simple Flat Laminate.

nodes are surrounded on all sides by exterior nodes and CVs. Exterior nodes are located on the outside surface of the laminate and set boundary temperature and pressure conditions for the laminate. CV top nodes retain their identity in the model and their x position, but move in the z direction based on compaction.

The model defines material properties for the resin and fiber. For each CV, its resin volume, resin pressure, permeability, temperature, viscosity properties are tracked over the course of the cure process. As shown in the figure, there are n x n =25 internal CVs representing the laminate. The notation for the external CVs is: left side CVs are numbered x=0, right side CVs (x=n+1), bottom CVs (z=0), and top CVs (z=n+1). The width of each CV is dx except for the left and right external CVs which are dx/2 and half CV volume. X(i) is nodal x position for CV(i,j). X(i) is at mid-CV width x-wise, except for (left and right) exterior CVs. Internodal distance is used for determining resin flow velocity and temperature conduction. For the exterior CVs, node position is on outermost side wall of CV. For a laminate that is rectangular, the same number of divisions is applied based on n. Therefore, dx will be greater than dz when the laminate length is greater that its height.

3.13 Tool Geometry and Contact

For the press cure process, the laminate is enclosed in a tool that constrains its dimension on the bottom and sides. The lid of the tool rests on the top of the laminate and provides the press temperature and pressure to the laminate upon contact. The lid is modeled as a separate body. Its geometry is 2D, defined in the x and y-dimensions without thickness in the z dimension. As the pressure cycle is applied the laminate is compacted and resin flows out its sides. The tool lid moves straight down in the z dimension with laminate height changes due to resulting resin flow. Contact of the lid with the laminate is detected by z position. When the gap between the positions of the laminate and lid is within a tolerance distance, then contact is defined as being made between the lid and top surface of the CV at that x-position. After contact is made, then pressure application and heat conduction to the laminate contacted CV surfaces is enabled. Laminate CVs adjacent to contacted CVs that are not in contact allow the resin to flow out of the top surface; otherwise, the path for flow is blocked.

3.14 Model Boundary Conditions

Exterior nodes and CVs are located on the outside surface of the laminate and set boundary temperature and pressure conditions for the interior CVs of the laminate. Given these exterior boundary conditions, the model estimates variable values within the laminate interior. The chief boundary conditions are pressure and temperature; all nodes/CVs that are on the external edge of the laminate are assigned values. The boundary condition resin pressure for the sides of the laminate represent the interface between the laminate and the bond tool. It is assumed that resin can flow out of this interface and the resin pressure there is set to zero Pa.

As the Lid makes contact with the laminate, the top CVs have pressure across their surfaces dependent on the applied force and the total laminate contacted area. The model assumes that all other CVs that are vertically aligned with the top contacted CVs share the same applied pressure. For monotonically increasing applied pressure conditions, the contact area increases, even though as additional contact area is gained, resin pressure may actually

decrease for CVs that were previously contacted. The applied pressure is equal within all CVs of the laminate when complete contact exist over the entire top surface.

Exterior CVs possess resin and fiber volume. Their heights and resin volumes are maintained in accordance with the resin flow volume rates, updating for each timestep. Thus they are kept at the same height as the adjacent interior CVs. Contact for exterior CVs on the left or right side is not defined per se. However, contact is defined as being true there if the adjacent interior CV is contacted. All resin flow out of and heat flow into the laminate is by way of the exterior nodes, depending on permeability and contact or not (Top CVs). exterior CVs at the bottom of the laminate are assumed to be in constant contact with the tool, and therefore no resin flow out of the laminate is assumed to occur there. Temperature for the exterior nodes is set to the tool temperature upon contact. It is assumed that most all of the prepreg material fiber orientation is in the length-wise (x) direction because of design loads that the part must sustain. Longitudinal permeability is defined as that along the direction of the fibers, in contrast to transverse permeability, which is oriented across the direction of the fibers. Because longitudinal permeability is typically 2 to 3 orders of magnitude higher than transverse permeability, the predominant resin flow direction is assumed to run across its length, with resin flow out the side edges. Since the resin pressures are defined as being zero at the edges, there will be a distribution of resin pressure along the laminate length, with the maximum at the length-wise center, and declining to zero at the edges.

3.15 CV Material Properties

The laminate model characterizes changes that occur during the cure process. However, CV properties are assumed to be uniform and constant during a timestep. These properties include resin pressure, permeability, resin viscosity, and degree of cure. Changes may occur based on resin flow and consolidation during the time step, and these changes are updated at the beginning of the next timestep. The height of a CV is assumed to be uniform across its width.

3.16 Contact Areas

Points of contact between the tool lid and the laminate are defined by position proximity. When the distance is within a tolerance of 0.000254 m (0.01”), contact is defined as true. A contact area is a group of adjacent contacted CV surfaces. It is assumed that uniform pressure is applied to all contacted CVs within the contact area, analogous to the flat laminate modeling situation. CVs at the edges of the contact areas are considered to be boundary CVs and are assigned a resin pressure of zero. The mid positioned CV(s) possess the maximum pressure, and all other CVs within the contact area are in-between. As long as a rigid lid is used that applies pressure uniformly over the contacted surface, the change in resin volume during consolidation will be the same, and shared equally for all contacted CVs.

For each timestep, the model scans the laminate surface x-wise for contacted CVs. The first and last CV that is contacted will constitute the exterior edges or boundary of the contact area. The applied pressure for the contact areas is the applied force/total contact area. The mid-length or center CV(s) for the contact area are taken as being representative of the consolidation state of the other CVs for the contact area. Its ESS is calculated, and with the applied pressure, the average resin pressure to apply for the contact area is determined. Pmax is calculated utilizing the distribution of resin pressure over the contact area CVs and assigned to the mid-length CV(s). Since the average resin pressure must be equal to the resin pressure determined from the ESS and the applied pressure, Pmax can exceed the average resin pressure. For each CV within a contact area, the model determines the unknown resin pressure for all remaining CVs, except the edge CVs, which are set to resin pressure of zero. All CVs aligned vertically with the contacted CVs are assumed to have the same resin pressure. The resin pressure gradient between Pmax and in the center of the contact area and zero at the edges produces a predominant resin flow that runs x-wise across the laminate from the center to its edges. The x-wise flows will be the same across each row of CVs, except for the top level CVs that have the opportunity for resin flow out the top. The flow volume rate per unit of time will be the same for each horizontal layer of the laminate, each layer contributing equally to the

total resin volume rate for the laminate. In general, for a flexbeam laminate, based on its geometry and the tool lid geometry, initially there will be 2 initial areas of contact with the laminate.

3.17 Flow Resistance

All resin flow between CVs occurs at the interface between the CVs; all resistance to resin flow is assumed to occur at these interfaces. All resin flow out of the laminate is through the exterior CVs. Therefore, the total resin flow volume rate leaving the laminate is the sum of the resin flow volume rates for the flow between all exterior CVs and their immediately adjacent interior CVs. The overall pattern of resin flow between CVs and out of the laminate for any timestep is modeled using a network of flow resistances and resin pressure. This approach ensures that all possible flow paths and volume rates for the given pressure gradients and conditions are considered in finding the equilibrium conditions at each timestep.

The total flow path for resin from the interior of the laminate to its edges is formed by a network of resistances, as illustrated in Figure 3.9. The notation for each CV and resistance uses i to denote x-wise position, and j to denote z-wise position, with x=0 being at the far left, and z=0 being at the bottom of the laminate. The predominant resin flows between adjacent CVs are assumed to run across CVs horizontally (with respect to the figure) and utilize a horizontal resistance (HR). Similarly, vertical flow is governed by a vertical resistance (VR). Each flow resistance is defined as a function of the variables in accordance with Darcy's Law: the minimum permeability between the 2 CVs, the average viscosity of the 2 CVs, the cross-sectional area, and the distance between the CVs. These variables are combined into a flow resistance value that exists between each CV that defines a network of resistances through which the resin flows, depending on resin pressure. The HR and VR are of the form:

- HR(i - 1, j) = (Visc(i, j) + Visc(i - 1, j)) / 2 * dx / (min(permL(i, j),permL(i-1,j)) / (FlowHgt(i - 1, j) * dy)
- VR(i, j) = (Visc(i, j) + Visc(i, j + 1)) / 2 * Abs(Z(i, j) - Z(i, j + 1)) / (min(permT(i, j),permT(i-1,j)) / (dx * dy)

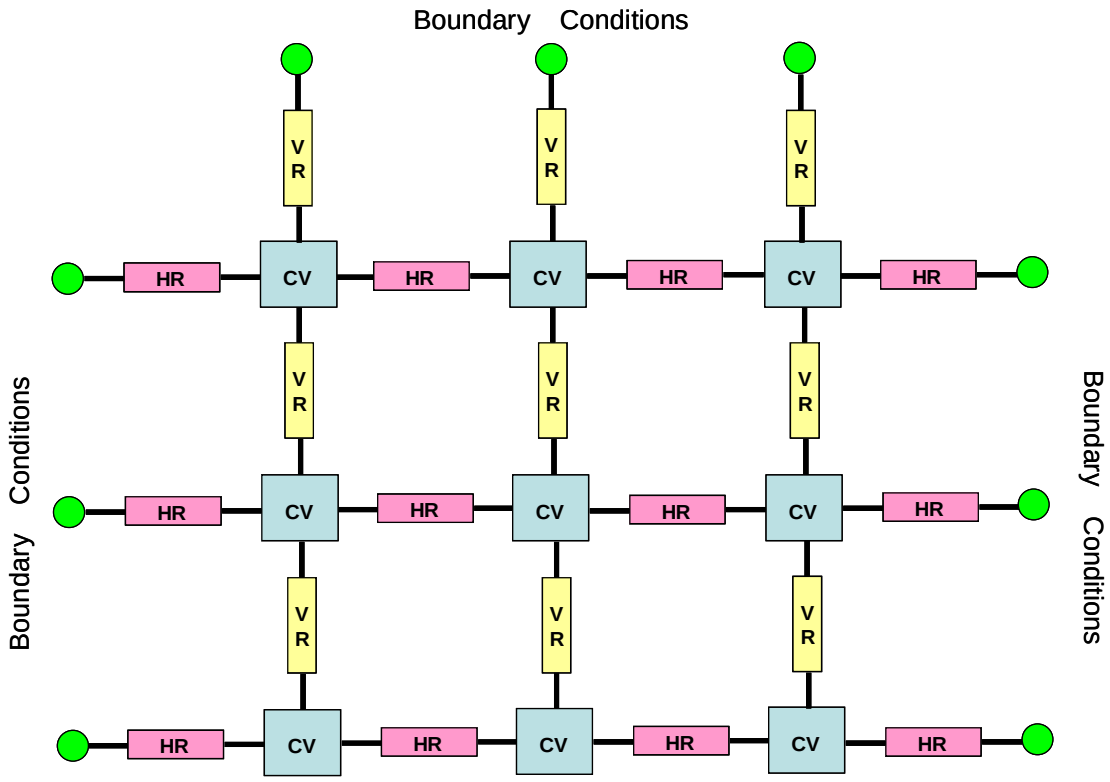

Figure 3-9. Flow Resistance Network Representing the Laminate.

where Visc(i, j) is the CV resin viscosity, permL(i, j) is CV longitudinal permeability, permT(i, j) is CV transverse permeability, dx is the typical distance x-wise between the CVs, Abs(Z(i, j) - Z(i, j + 1)) is the vertical distance between the CVs, and FlowHgt(i,j) is the common CV height between CV(i,j) and CV(i+1,j). Note that the HR values incorporate longitudinal permeability and VR values incorporate transverse permeability. The cross-sectional area (flow channel) through which resin can flow between 2 adjacent CVs is the flow height * dy. Since resin viscosity may differ for the 2 CVs involved due to temperature effects, the average viscosity of the 2 CVs is used for the resin flow between them. The more restrictive minimum permeability between the 2 adjacent CVs value is used.

The resin flow for the contact areas is assumed to follow across, with flow moving to the left and right from the x-wise center/mid CV to each edge. The resistance to resin flow depends on the state of all the CVs the resin must pass through on its way out. This is analogous to 2

series electrical circuits—a left and right- at each j level of the laminate, where the left or right flow volume is the same for all CVs to the left or right. Thus an equivalent resistance can be computed that determines the left and the right flows. Each CV has a pressure drop across it depending on the flow and the CV's resistance to flow. The resin flow to the edge CVs from their adjacent CVs within the contact areas will be utilized to measure the resin flow volume rate leaving the contact area. The resin flow volume rate (cubic meters/second) between any 2 CVs is then delta RP/resistance.

3.18 Flow Volume Rate and Pressure Drops

The model uses Darcy's Law (an analogy to Ohm's Law) to determine the resin volume rate between any 2 CVs. If CV(1) has resin pressure RP1 and CV(2) has RP2, for a given cross-sectional area, then the resin volume rate (RVR) in cubic meters per second between the CVs is given by

$$RVR_{12} = \frac{RP_1 - RP_2}{R_{12}}$$

where R_{12} is the flow resistance between the 2 CVs. For the flat laminate situation, a rigid lid imposes uniform pressure across the entire top surface of the laminate causing resin flow. If all CVs have uniform material and flow resistance properties, the total resin volume rate flowing out of the laminate is equally contributed by each CV. Therefore, the predominant flow running across a row of CVs (as in the figure) is equal and the resin pressure for a CV is a function of the flow rate and its distance or total resistance from the edge. For this common flow rate running across this series of CVs, there is an equal pressure drop or gradient across each CV. Each contact area for a laminate follows these same conditions as for the flat laminate.

3.19 Solving for Unknown Resin Pressures

The model utilizes Kirchoff's law to determine the unknown resin pressure values that result from resin flow through the network of flow resistances that represents the laminate. CV resin pressures range from zero at the edges to Pmax at the center. Note that the model does not use this approach when all CV resin pressures are known, i.e., when the tool lid makes

contact with the entire laminate top surface. It will be assumed that once all top CVs are contacted that all CVs within the laminate will have the same P_{appl} conditions based on total contact area and applied force. ESS will then be determined based on V_f for each individual CV. Pressure and resin flow is modeled using an electrical current and voltage analogy. Kirchoff's Laws for voltage and current require that at any node or circuit junction, as in Figure 3.9, the sum of all current drops must equal the sum of all voltage sources. Taking resin pressure as an analogy to voltage and pressure drops as an analogy to current drops, a Kirchoff's law algorithm is applied to determine the unknown resin pressures and resin flow rates within the network at equilibrium for each timestep of the simulation.

3.20 Description of Kirchoff Algorithm

The Kirchoff algorithm used in the model is based on the method described by Carnahan (1969). The equations that relate resin pressure at the nodes/junctions of the network can be found by applying an analogy to Kirchoff's Current Law: the sum of the flows arriving at each node must be zero. Application of these laws leads to a system of flow conservation equations, one for each node in the network. An augmented matrix is used that contains the coefficients of the unknown laminate interior CV resin pressures. The right hand side (RHS) of the matrix is a vector holding the constants associated with each node being evaluated. Row k of the coefficient matrix contains the coefficients for the node being evaluated and the coefficients for its neighboring nodes. Referring to the network in Figure 3.9, for any node or junction there are either 3 or 4 possible paths or legs for resin flow to follow. That is, for an interior node, there is a path for flow to its left, right, below, and above, for 4 leg flow pattern. For bottom nodes, a 3 leg flow pattern applies. For each 3 leg and 4 leg flow pattern, different expressions were developed for the coefficient of the node being evaluated, as well as the node to left, right, below and above (as applicable).

The model code assigns a k value uniquely to each interior node that will be evaluated. As each node k is evaluated, the coefficient values for node k and its neighboring nodes are placed in the proper column of row k of the coefficient matrix. Coefficient(row, col) is used to

hold these values, with R(k) being used to hold the RHS constant for row k. The Gauss-Jordan algorithm from Chopra (2005) is used to solve for the unknown CV resin pressure values. When a resin pressure is known, that value is used to generate a pressure drop that is transposed to the RHS.

3.21 Flow Direction Monitoring

It is suspected that the direction and magnitude of the resin flow is critical, and changes to either/both may signal the conditions for fiber waviness. For each CV, the model monitors per time its resin flow rate and direction so that significant changes to magnitude and direction can be detected. A flow direction sign convention (- and +) is used to indication flow from the center of each contact area towards the left or right side, respectively. When additional CVs become included in a contact area, the flow direction exiting a particular CV can reverse. The magnitude of colliding resin flow directions is given a value that is monitored as a possible condition for fiber waviness to occur. The model supports multiple possible contact areas as well as the initial 2 on which the tool lid rests on the laminate top surface at time = 0. It is expected that both these 2 possible contact areas will expand in area with laminate consolidation, ultimately becoming a single contact area covering the entire laminate top surface.

3.22 Summary of the Consolidation-Resin Flow Submodel

The following bullets briefly describe the highlights of the composite laminate consolidation-resin flow submodel. The next section presents the sequence of execution of steps for the model software code.

- The resin pressure, permeability, height, viscosity, and other properties are assumed to be uniform within any CV.
- The Pappl to any CV or contact area is = Force/contact area.
- For any CV, Gutowski's expression gives the resin pressure as a result of Pappl and the current ESS.

- All vertically aligned CVs with the contacted ones have the same resin pressure. So, in general the flows across each j level are the same, except for top CVs that have opportunity to flow out the top. The flow volume rate per unit of time will be the same for each horizontal layer of the laminate, each layer contributing equally to the total resin volume rate for the laminate.
- All resin flow between CVs occurs at the interface between the CVs; all resistance to resin flow is assumed to occur at these interfaces. The sum of resin flow to the exterior CVs from each immediately adjacent interior CV is the total resin flow leaving the laminate. The total resin flow volume rate leaving the laminate is the sum of the resin flow volume rates for the flow between all exterior CVs and their immediately adjacent interior CVs.
- The resistance to flow at the interfaces is a function of min perm among the 2 CVs, average viscosity of the 2 CVs, common height between the CVs (* dy to form a flow channel area), and the space between.
- The resistance to flow defines each horizontal resistance HR, and vertical resistance VR.
- The resin flow volume rate between any 2 CVs is calculated by dividing the resin pressure gradient by the resistance to flow in accordance with Darcy's Law.
- With horizontal flow and the pressure drops for the flat laminate situation, an equal contribution of resin flow volume rate from each CV is assumed. Therefore, for a series of CVs with a common flow, there is an equal pressure drop across each CV, since each CV has the same flow volume rate and material properties for each CV in series.
- Since the average resin pressure must be equal to the resin pressure derived from Gutowski's ESS and Pappl expression, the Pmax will exceed the average resin pressure.

- Resin pressure causes resin flow and increases in V_F. Each CV may differ in V_F depending on how much net flow out has occurred.
- Resin pressure will decline when Pappl is not monotonically increasing, using a pressure film approach.
- The flat laminate flow properties can be extended or apply as well to contact areas—i.e., same total flow volume rate and distribution of resin pressures.

In summary, the solution via the Kirchoff algorithm for resin flow rates and resin pressures at the nodes/junctions is based on the flat laminate mode. A rigid lid surface imposes uniform pressure across the laminate top surface causing resin flow. All laminate volume is assumed to consist of fibers fully saturated with resin, with negligible void volume. Resin volume flowing out the sides is contributed equally by all sectors of laminate resin volume. Therefore, assuming homogeneous material properties throughout, resin pressure ranges from zero at edges to Pmax at the center.

3.23 Flow Chart/Sequence for the Flexbeam Model

1. Setup model, initialize variables, definition of laminate CVs and nodes, material properties, etc.
2. Define initial location of laminate surfaces and lid surfaces; determine contact (true/false).
3. Set current time, read current cure cycle conditions- including force.
4. Update model status- update laminate heights, resin volumes, V_F, node locations, lid position. Update contact status of each CV.
5. Determine flow heights for all CVs – update based on changes to heights from change in resin volumes. Then using this value as input, determine flow resistance values HR and VR. VR for flow out top of top level CVs is dependent on contact or not.
6. Define contact area(s) and mid-contact area CVs for Pmax determination-- based on current contact areas, set holder for Pmax value for the mid- contact area CVs- this includes setting single CV for odd numbered CVs within a contact area, or setting up 2 mid-

length CVs for an even number of CVs within a contact area. Correct Pmax to be calculated later to replace these values.

7. For each CV with holder resin pressure assigned, determine Pappl and resin pressure based on CV's current ESS and V_F. This resin pressure value to be target average resin pressure to be calculated for all contacted CVs within each contact area. Note: if all CVs are contacted then AllContact (Boolean) is true, and all these CVs are treated as a single contact area.
8. Determine Pmax for each contact area - set Pmax for only laminate top surface j=n+1 CVs. Then set all other j level CVs to top level values.
9. At this point all CV resin pressure should be defined—Pmax for mid-contact area CVs, 0 for edges of each contact area, and "" i.e., unknown, for in-between CVs. Submit these values to Kirchoff algorithm for solution: determine resin pressure for all CVs based on flow that results in equilibrium pressure drops and resin pressure for the flow resistance network.
10. Determine resin flow volume rates for each CV (cu meters/sec).
11. Determine flow direction for each CV. Alert through display any detected changes in resin direction.
12. Determine temperature distribution, and update degree of cure, resin viscosity for each CV.
13. Update time + continue. Update each CV status.

3.24 Cure Kinetics Models

The cure kinetics model used for the 3501-6 material is the nth order formulation:

$$\frac{d\alpha}{dt} = Ae^{-E_a/RT}(1-\alpha)^{NC}$$

where α is cure, A is the pre-exponential factor, E_a is the activation energy, R is the universal gas constant, T is absolute temperature, and NC is the order. The cure model used for the 8552 material is the autocatalytic formulation:

$$\frac{d\alpha}{dt} = A_n e^{-E_a/RT}(1-\alpha)^{NC}(\alpha)^{NC2}$$

where α is cure, A_n is the pre-exponential factor, E_a is the activation energy, R is the universal gas constant, T is absolute temperature, and NC is the order.

3.25 Material Model Parameters

Table 3-1 presents the material property constants used for the model. The resin cure kinetics and viscosity model parameter values for each material used are summarized in Table 3-2.

Table 3.1. Material Property Constants.

Material	IM7/3501-6	S2/8552
Conductivity (W/min-K)	0.574	0.574
Specific Heat (W/Kg-K)	862.1	889
Density (Kg/m^3)	1557.7	1831.3

Table 3.2. Cure Kinetics and Viscosity Model Parameters.

Parameter		Material	
Name	**Description**	**IM7/3501-6**	**S2/8552**
A1	Pre-exponential factor 1 (/min)	5.027E16	3.533E12
A2	Pre-exponential factor 2 (/min)	3.637E10	98160
EVOR	Activation energy 1 (J/℟)	28216	25000
EVOR2	Activation energy 2 (J/℟)	22104	11846
NC	Order component 1	2	2
NC2	Order component 2	1.5	0.5
HU	Ultimate heat 1 (J/Kg)	5154.56	155145
HU2	Ultimate heat 2 (J/Kg)	193850	58848.3
VM	Maximum viscosity (Pa-secs)	2.98E-22	0.01
KV	Pre-exponential factor (/min)	25.71	8.235
EVOR	Activation energy (J/℟)	32542	8024

CHAPTER 4

RESULTS

4.1 Overview

The cure and consolidation of a representative rotorcraft flexbeam composite laminate is a formidable process and the model described in Chapter 3 was aimed at being simple while capturing its essence. The model integrates the thermal behaviors of heat transfer and generation emanating from press tool contact with resin pressure and flow. A representative composite flexbeam part and press tooling was designed to demonstrate the cure process. Each control volume (CV) comprising the part embodies the required fiber and resin properties. In response to tool contact force, resin pressure is increased, causing flow through the network of flow resistance of each CV within the laminate to exit out the edges. As each CV loses resin content, the increase in fiber volume fraction is monitored. Laminate consolidation takes place as the tool lid and containment pushes resin out and the laminate becomes more dense. In accordance with changes in permeability the resistance to flow increases exponentially while a nonlinearly increasing proportion of the applied force is imposed on the fibers in relation to the resin. The thermal behaviors include changes to the resin as viscosity is reduced during heat-up, accompanied by onset of the cure reaction. The resin cure kinetics submodels for 8552 and 3501-6 characterize this evolution leading to a permanently hard glassy solid. In some regions of the laminate, especially adjacent to outside edges, a resin-poor condition may be present due to flow, leading to increased void volume.

The flat laminate model portrays the changes to resin pressure, resin flow, volume change, and consolidation due to a constant load being imposed on the laminate top surface. This model was validated by comparison with Hubert's (Hubert, 2001) original experimental data and results. The compaction curve describes the relationship between the applied force and laminate height as it consolidates over time, subject to fiber and resin properties and

temperature conditions. The principles of the flat laminate model were then carried over to each CV of the larger flexbeam model.

Once the flexbeam model was built and the software functionality verified, the numerical values that it produced were checked and validated before the model was utilized for experimental optimization iterations. The cure and viscosity model predicted values for S2/8552 were evaluated first. Estimated degree of cure values from the cure model were acceptable. The minimum output value for viscosity was compared with Hubert's minimum value of 3 Pa-secs when subjected to a straight temperature ramp of 2 degrees C per minute. The flexbeam model was run and attained a minimum viscosity value of 2.5 Pa-secs, deemed acceptably close. Likewise, good agreement was found with the IM7/3501-6 cure and viscosity model values.

4.2 Model Operation

One of the first checks for fidelity of the model was to verify tool lid movement and subsequent contact with the flexbeam laminate. Figure 4.1 displays the side view of the tool lid

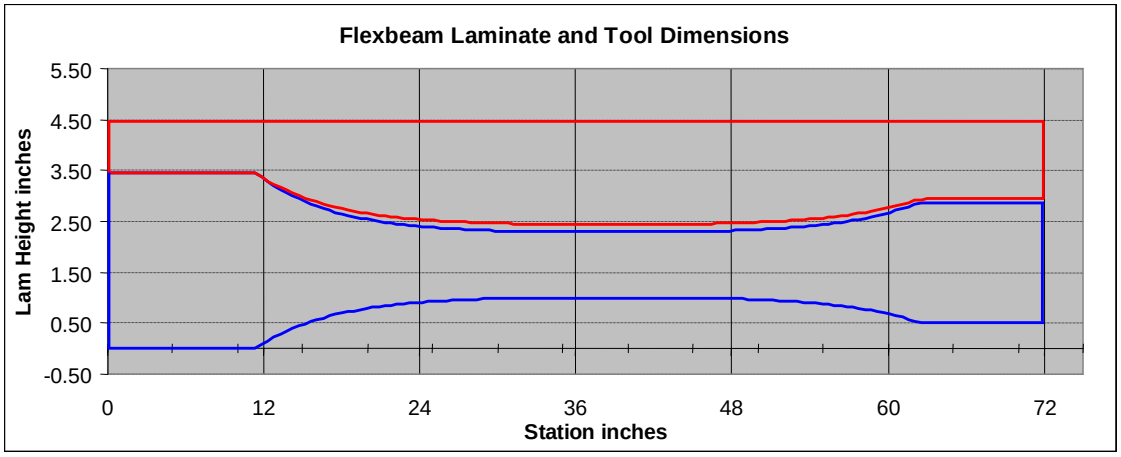

Figure 4.1. Lengthwise View of Tool Lid (red) Contact with Flexbeam (blue).

and flexbeam laminate. Figure 4.2 illustrates a 2-dimensional view of contact between the tool lid (fushia) and the flexbeam laminate (blue) over CV nodes along the flexbeam length (x) and height (z) at time = 0. As it indicates, the initial position of the lid is resting on two small contact

areas of the flexbeam top surface. As heat and pressure is applied to the contacted surfaces, resin flow out of the laminate reduces the height of the top surface, bringing about increasing lid contact.

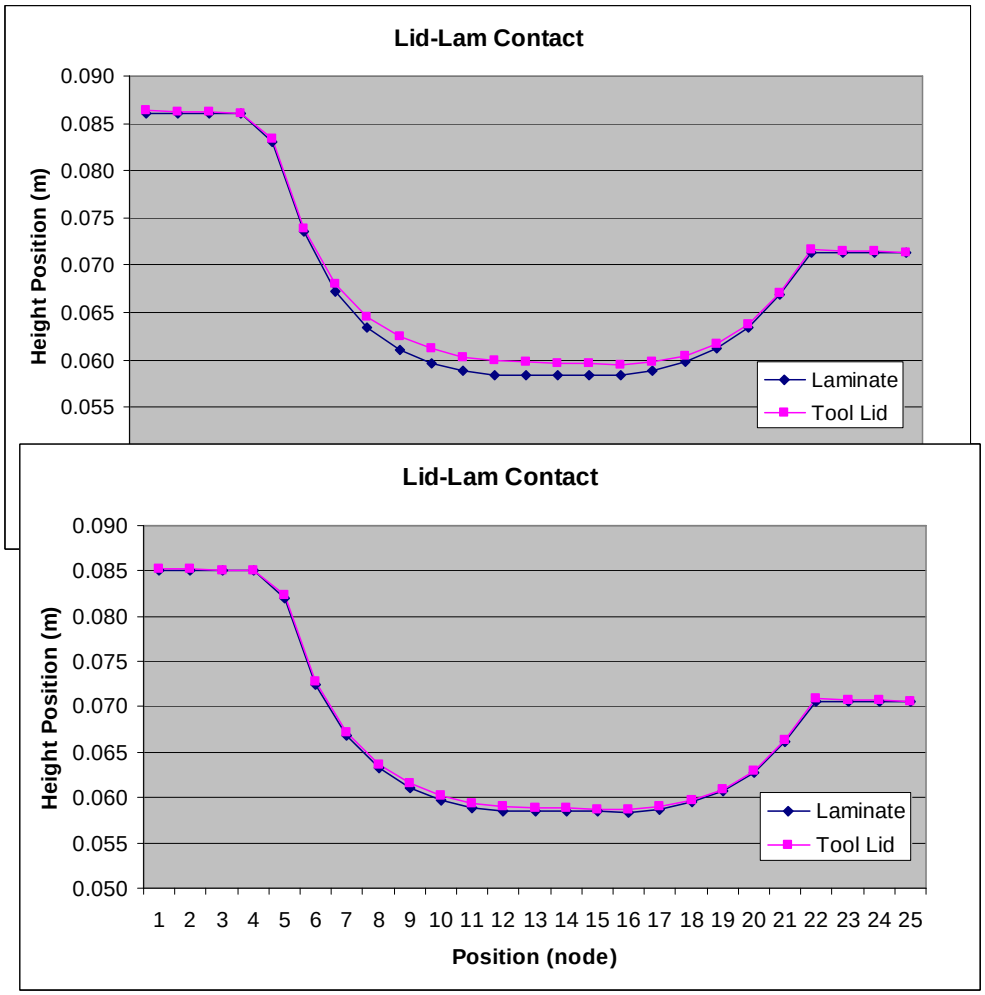

Figure 4.2. Progressive Lid Contact with Laminate.

4.3 Thermal Cycle Optimization

The first consideration for cure process optimization is control of laminate temperature, since the temperature schedule paces the entire cure process time. Pressure is applied under appropriate resin state conditions, and is completed within the temperature schedule timeframe. The laminate temperature is driven by changes in tool temperature vs. time during the cure

cycle. The ability to optimize temperature for a laminate that is 3.45” thick (at the root end) is a challenge; the highly interactive and nonlinear nature of the laminate’s thermal state with its reaction rate made finding an optimum a relative choice based on what constraints are imposed. The following groundrules were established:

- A maximum laminate temperature of no more than 180℃
- A maximum temperature difference within the laminate of 10℃
- A dwell at 177C for 2 hours to complete cure

Conventional industry practice for a cure cycle is to increase temperature from ambient via an initial ramp, of perhaps 0.1 C per minute, to an intermediate temperature within a range of 80 to 100C, followed by a dwell there of 120 minutes, then again ramping to the final cure temperature of 350F/177C. In order to optimize the cycle time, greater ramp rates are used; however, as it is increased, the temperature difference within the laminate increased. One of the constraints for an acceptable flexbeam laminate in terms of strength is limiting this difference. The purpose of the first ramp is to get the laminate to a state where pressure application can be completed while maintaining uniform cure and viscosity within the laminate. The dwell is used to allow the laminate cure and viscosity to become as homogeneous as possible, so that effects of the pressure application will be consistent throughout.

For the S2/8552 flexbeam, multiple attempts were made using the model to simulate the process. The tool temperatures were manipulated through the simulation, while the temperatures of the exterior laminate surfaces in contact with the tool bottom, sides, and lid followed the tool temperatures. The first attempt using common industry practice resulted in a reasonable overall cure time of about 14.5 hours, but with excessive temperatures (unacceptable maximum temperature of approximately 216C) and exotherm. After all, this is a very thick laminate, and the energy to be released during cure is formidable. Note that the following figures, beginning with Figure 4.3, do not show the time in the cycle for cool-down following the dwell at the final temp of 177C.

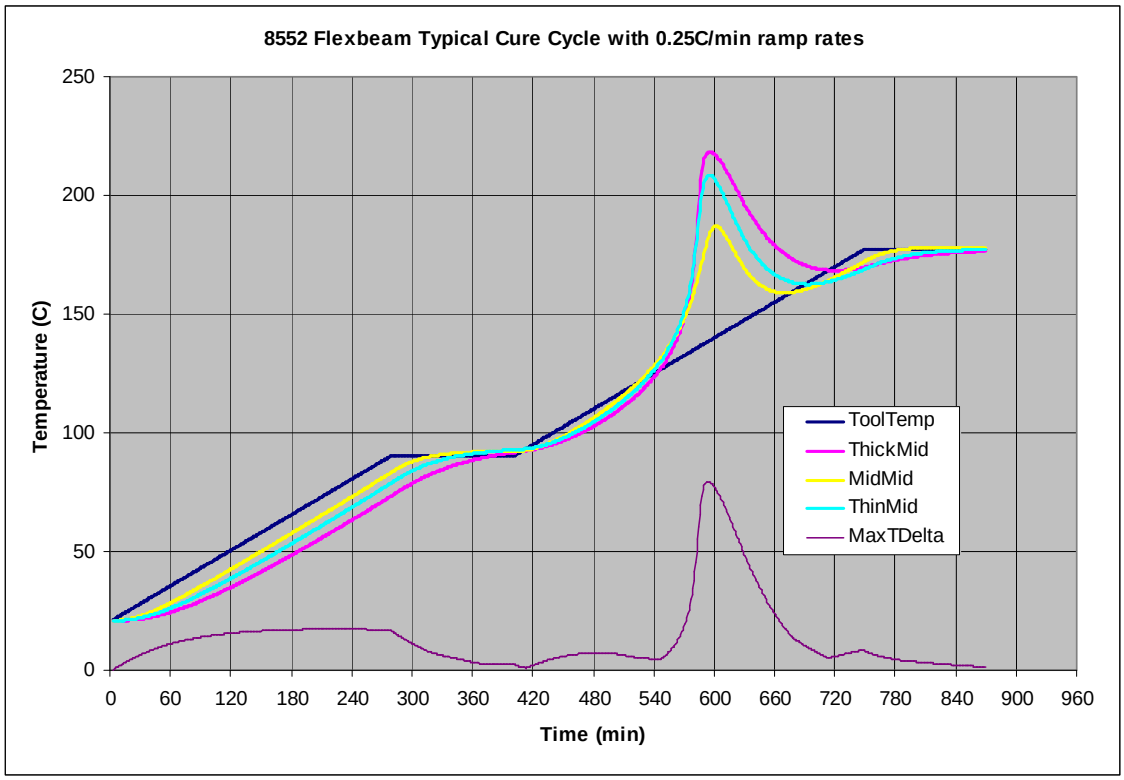

Figure 4.3. Conventional Approach using Two Temperature Dwells.

In the second attempt, additional dwell temperatures were added at 100, 120, 140, prior to the 177℃ dwell. This attempt, summarized in Fig ure 4.4, yielded obvious violations of the constraints: a maximum temperature of 175℃, with a maximum temperature difference within the laminate of 54℃. Again, this was an unacceptab le cure process.

4.4 Thermal Cycle Optimization Approach

The second objective of this research was to apply the model within an optimization scheme to determine the most time-efficient cure cycle processes. Optimizing the cure of a thick laminate differs considerably from a thin laminate often cited in the literature, for which the conduct of its cure is relatively straightforward. The interactions of temperature ramp rates, current laminate degree of cure and its resulting reaction rate were found to be highly complex. Given the thickness of the 8552 flexbeam, in seeking to increase temperature as rapidly as possible in order to shorten overall cure process time, significant temperature differences were

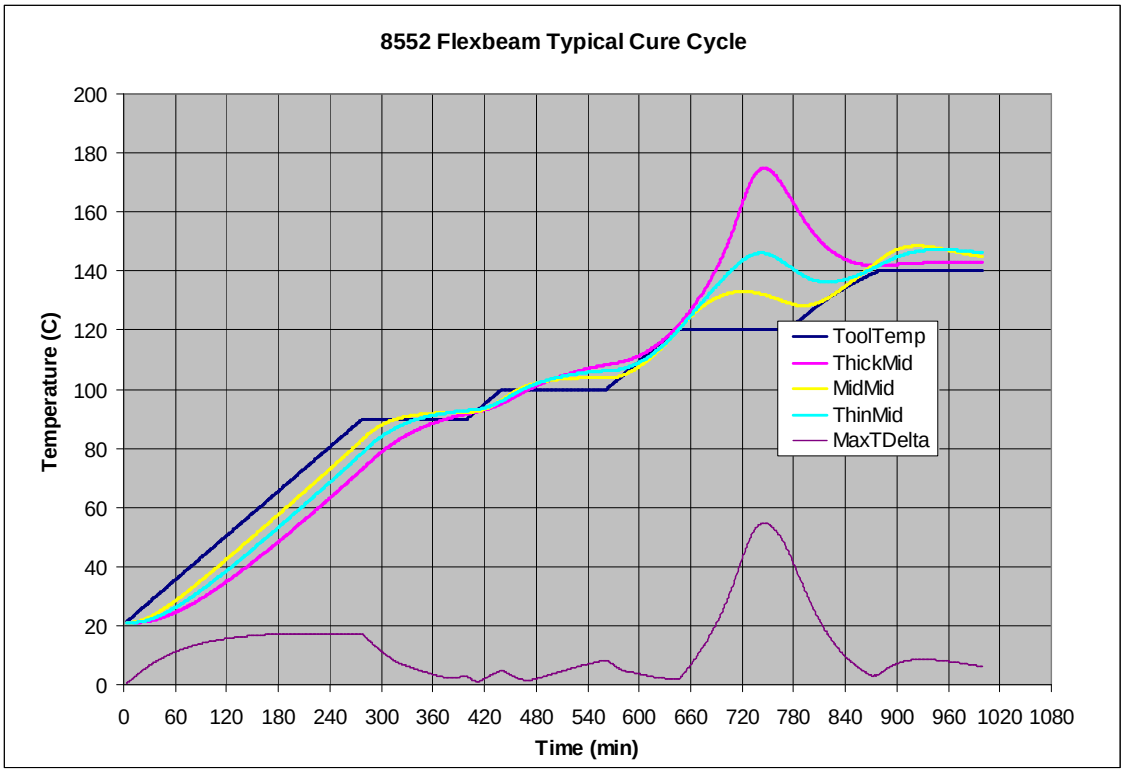

Figure 4.4. Second Attempt at Thermal Cycle Using Multiple Dwells.

incurred within the laminate. Therefore there can exist major differences in degree of cure and cure rate within local regions of the laminate. At the thick end, the maximum temperature difference exists. The thinner other end has the 2nd most temperature difference, followed by the thinnest mid-length region. Keeping the maximum temperature within the laminate within a few degrees requires that the temperature ramp rate be small, significantly extending the overall cure cycle time.

Because of the sensitivity of the material to exotherm and loss of control, a self-directed approach using the cure rate was selected to seek optimization of this process. This approach varies the tool temperature rate, upon which the laminate temperature depends, subject to the maximum temperature difference within the part. A future cure rate was assessed for various future times before settling on 90 minutes ahead as the most useful. The algorithm projects out into the future the current temperature rate to arrive at a future laminate temperature. A

maximum future cure rate value is determined by the cure kinetics model and this is used as a proportional feedback to the temperature rate. Figure 4.5 indicates how the cure rate was used to slow down the heat up rate during the ramp from 90 to 177℃. Rather than following a constant rate for the second ramp the tool temperature rate was altered based on the predicted cure rate. Using the constraint of <10℃ maximum de lta temperature as well as < .001 degree of cure per minute looking 90 minutes into the future, an acceptable cure cycle is shown in Figure 4.6. Note that now, in order to satisfy the constraints, the overall time has been extended to about 37 hours.

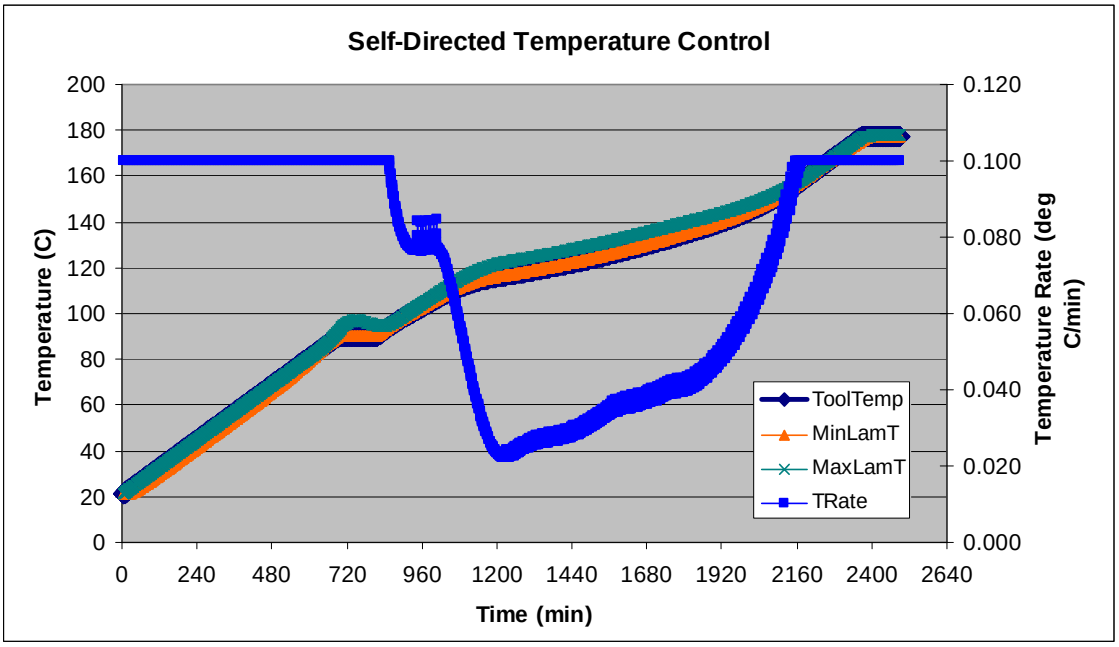

Figure 4.5. Application of Self-Directed Temperature Control using Estimated Future Cure Rate.

Rather than employ a limited number of temperature piecewise linear stages with their respective durations as was done by Rai et al (Rai, 1997) in seeking the optimal temperature cure cycle, here an algorithm was employed that seeks the maximum temperature rate setpoint for each minute, constrained by the maximum temperature difference within the laminate and the estimated cure rate at 90 minutes into the future. If either of these are in excess/exceed the

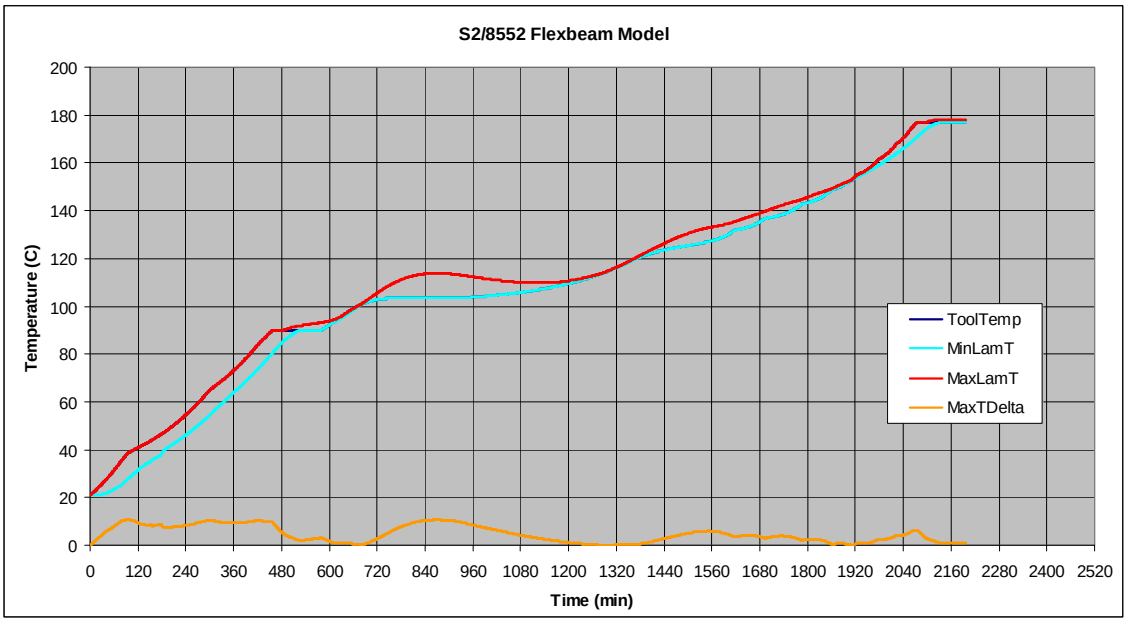

Figure 4.6. Acceptable S2/8552 Flexbeam Temperature Cycle.

constraints, the next temperature setpoint is reduced, and so on for each next minute. This is equivalent to having many more individual temperature stages using the Rai model.

The groundrules that were specified for temperature optimization served as basic rules or constraints applied to the self-directed control approach to find a reasonable optimum cure process. Thus the constraints act as rules that guide the "controller" at each timestep, effectively paring down the optimum domain space by eliminating from consideration those values that would violate the constraints. While not guaranteed to be the global (which is improbable) optimum, it is assured to be a local optimum cure process.

For the 3501-6 flexbeam laminate, a similar course of action was followed, in order to arrive at an acceptable temperature cycle, subject to the same constraints of maximum temperature and maximum temperature difference within the laminate. These results are presented in Figure 4.7. Note that the total process time to complete the 177℃ dwell is 35 hours, less than the S2/8552 flexbeam laminate.

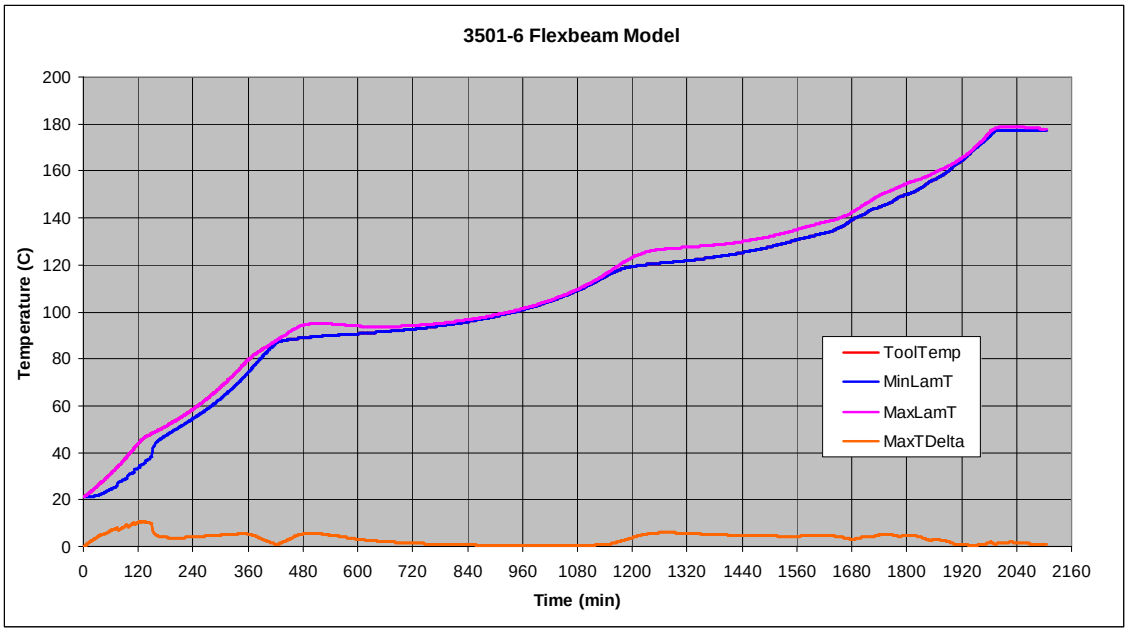

Figure 4.7. Acceptable IM7/3501-6 Flexbeam Temperature Cycle.

4.5 Pressure Application

Having established an acceptable cure cycle for thermal requirements, especially not exceeding the bounds of temperature difference, concern was shifted to the pressure application. First, in seeking the appropriate final pressure level, there is a range of target FVF for the flexbeam part for it to possess optimal strength. Too little resin surrounding the fibers detracts from strength; if not enough resin is pushed out during consolidation, there is a danger of inadequate cohesion between the cured resin and the fibers, with voids possibly in the midst. Standard industry practice suggests these final FVF target ranges: for S2/8552, 52% and for IM7/3501-6, 63%. Note that the starting FVF used for the model for S2/8552 is 48%, and for IM7/3501-6, 51%. For both materials, the final level of force applied to the designed flexbeam was set at 769,000 Newtons, appropriately equal to 400 psi.

For the pressure application during the cure cycle, an industry rule of thumb was used for the pressure cycle: ¼ of the final pressure level was applied at t = 0, and the remainder applied through a 5 minute ramp when the resin state was suitable. Heuristic-based guidance is

useful; as pointed out by Ciriscioli et al (Ciriscioli, 1990), the resin state must be uniform as pressure is applied to assure that pressure effects on resin flow throughout the laminate are also uniform. While observing the viscosity changes due to cure and temperature changes, it starts at a high level (37588 Pa-secs for 8552, 10059 for 3501-6) and progressively decreases as laminate temperature rises and cure initiates. However, due to the temperature ramp and the temperature differences in the laminate, there is also a viscosity difference in the laminate that is ideal/conducive/desirable/ to pressure application. (The initial pressure value only used to ensure adequate contact between the lid and laminate for heat transfer.) As temperature reached something of a plateau due to the laminate temperature difference constraint, the temperature and viscosity differences progressively decrease. A viscosity difference value of 7 Pa-secs was chosen as a gate or condition or system state at which pressure ramp can start. This condition is accompanied by a minimum viscosity condition, by which the least pressure is required to induce resin flow on its path to reaching the final target FVF. The resulting cure cycle is shown in Figure 4.8.

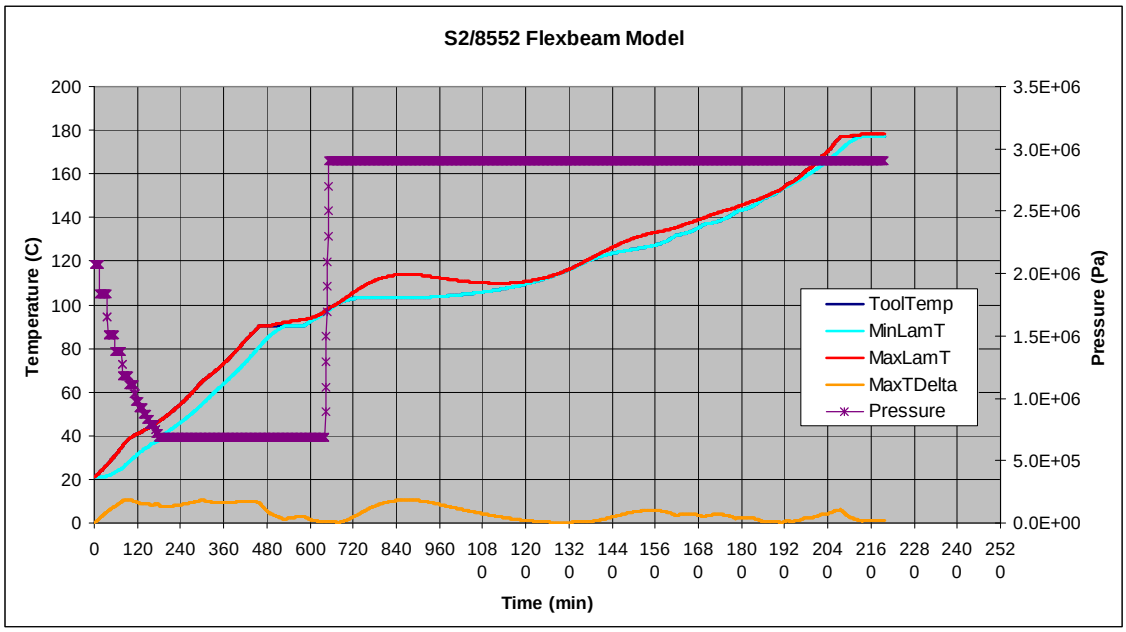

Figure 4.8. S2/8552 Flexbeam Cure Process with Pressure Application.

Note that while the force is held constant from t=0 until around t=180 minutes, the pressure on the laminate drops, caused by progressively more contact area between the tool lid and the laminate. As the resin melts due to heat transfer more resin flows out of the contacted CVs, and these CV heights are reduced, allowing the lid to contact more top surface area.

4.6 Investigation into Material Property Variation

Variation is a known factor affecting yields of composite parts. For a closed-cavity, press cure process, it is suspected that variation in per ply thickness, caused by varying thickness of resin film, along with process variation during the prepregging process. The result of this difference in bulk is that for a fixed number of plies in a laminate layup, the thicker regions will vary disproportionately, causing a change in the initial contact patterns between the tool lid and the laminate top surface. This change is suspected to cause differences in resin pressure patterns as a result, which may affect the tendency for fiber waviness to occur. For each flexbeam material, two levels of bulk were applied with the model, 10% and 15%. The output data for each case was then analyzed.

4.7 Model Output For Cure Process with a Symmetric Laminate and Tool

Before presenting the results for the designed flexbeam and tooling, if the flexbeam laminate and its tooling were instead symmetrical with respect to length, the expected pressure distribution would also be expected to be symmetrical. As a check, the laminate and tool geometry were adapted to be symmetrical. Figure 4.9 illustrates the initial contact positions of the flexbeam and tool lid.

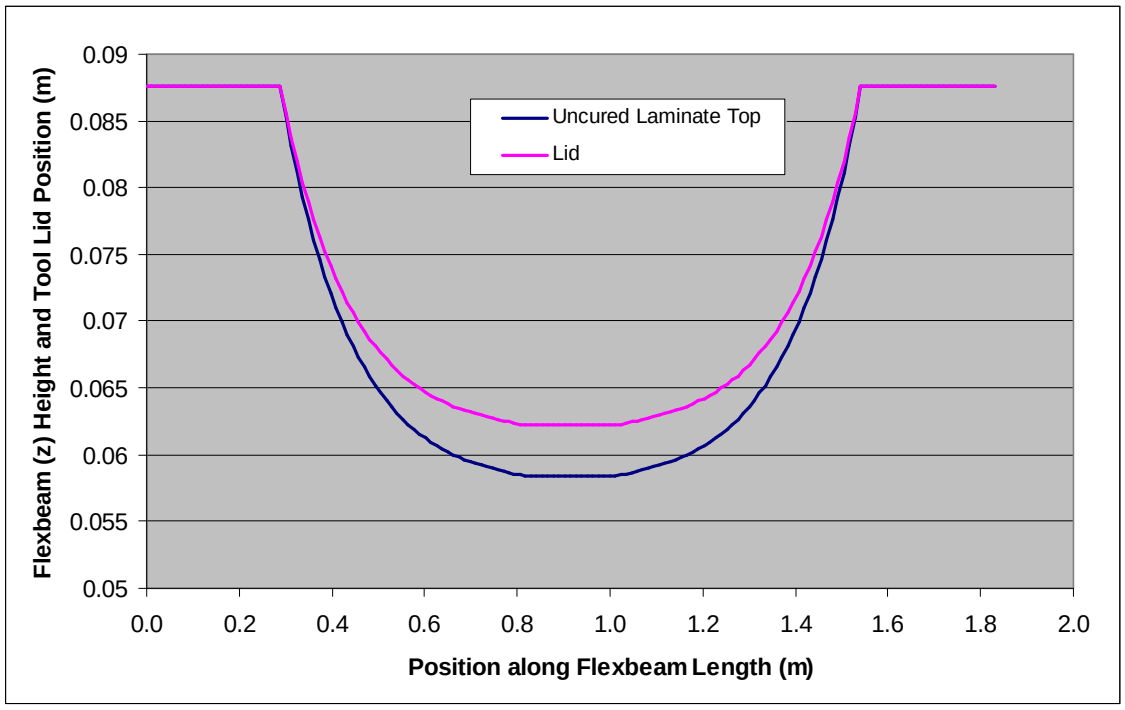

Figure 4.9. Initial Lid/Laminate Contact.

The predicted resin pressure distribution along the flexbeam length at t=5 minutes is presented in figure 4.10. Figure 4.11 presents the estimated resin pressure distribution at t=214 minutes, when all but the center regions have established contact between the laminate and the lid. Note that both figures portray a symmetrical pressure distribution, as would be expected from a symmetrical laminate and tool lid model. Because the resin flow direction from each of the contact areas on each end of the laminate is towards the center, the model predicts that a collision will occur between these opposing flows.

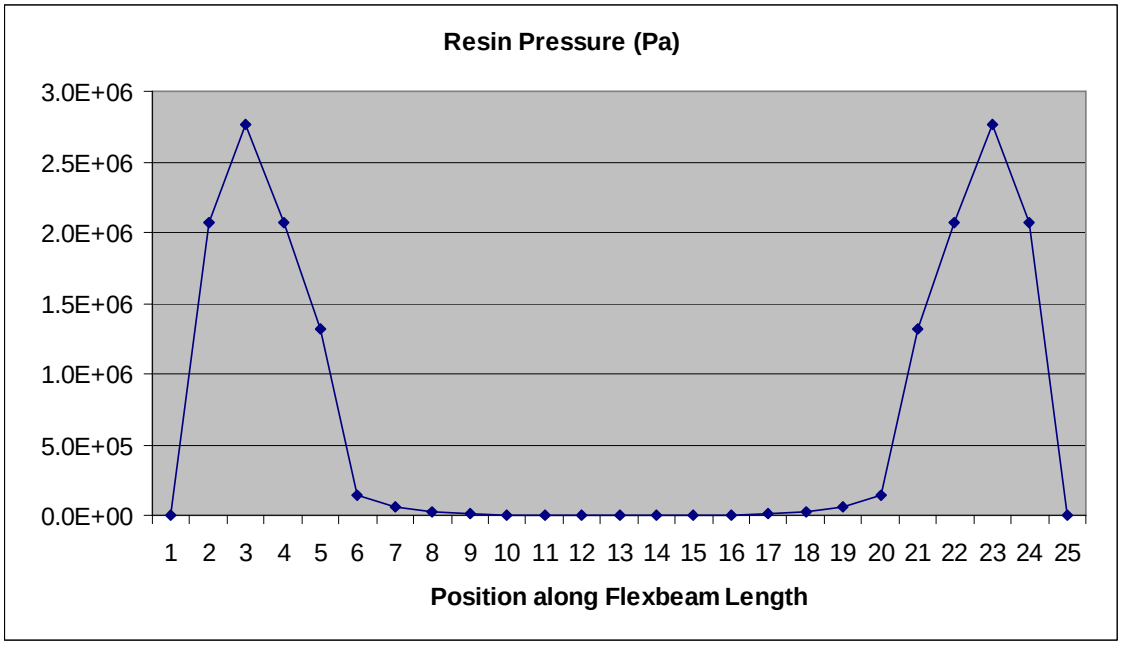

Figure 4.10. Estimated Resin Pressure Distribution at t=5 Minutes.

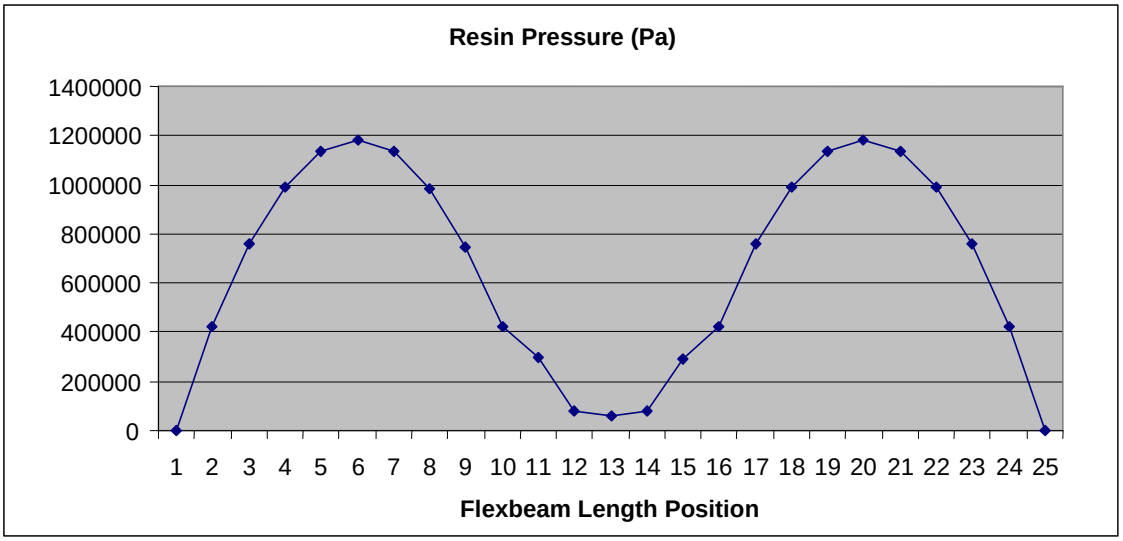

Figure 4.11. Estimated Resin Pressure Distribution at t=214 Minutes.

4.8 Model Output For Cure Process-- Suspected Origins Of Fiber Waviness

The flexbeam model produced many indications that it was a representative model. Using the reasonably optimized S2/8552 flexbeam thermal cycle, it was noticed that until about

55 minutes into the S2/8552 cycle, there was no resin velocity in the center (with respect to length of the flexbeam). With the passage of simulated time, as the thermal contact was maintained over the two initial areas of contact, the contact areas increase in size, and the resin temperature gradually increases in the center regions, and with it the viscosity decreases, enabling resin flow across the entire length.

For the S2/8552 flexbeam during the cure process 5 minutes before the point in time when the tool lid will make contact with the entire laminate surface, Figure 4.12 portrays the distribution of resin pressure along the flexbeam length. The model portrays the twin peaks of resin pressure emanating from the contact areas between the lid and the laminate. Figure 4.13 displays the resin pressure distribution at the time of full contact being achieved.

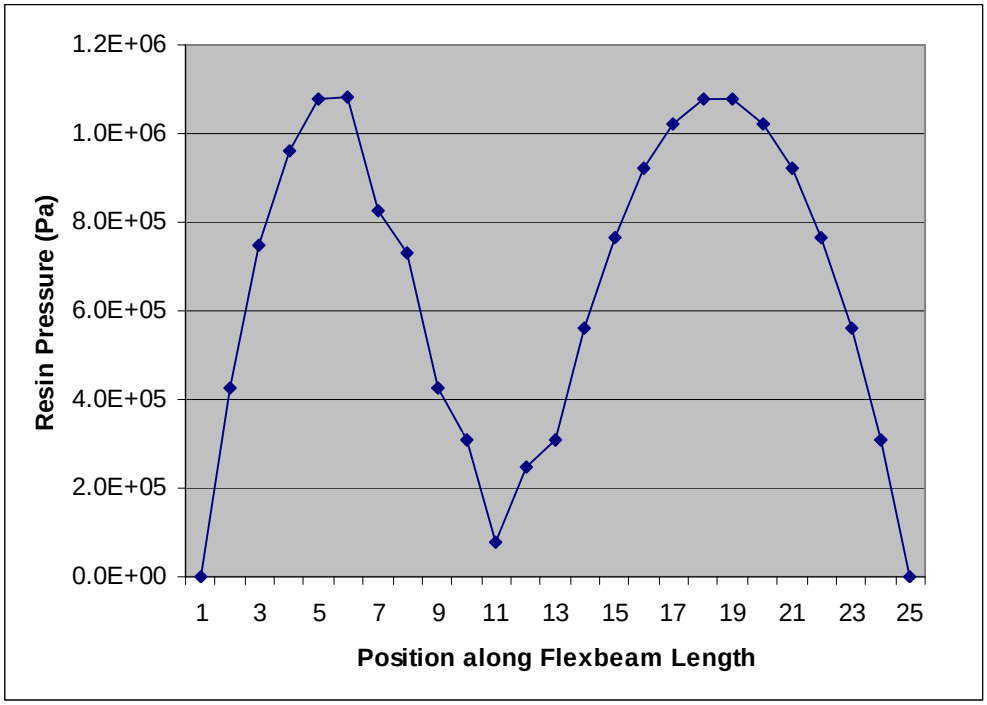

Figure 4.12. Resin Pressure Distribution Just Before the Time of Full Lid/Laminate Contact.

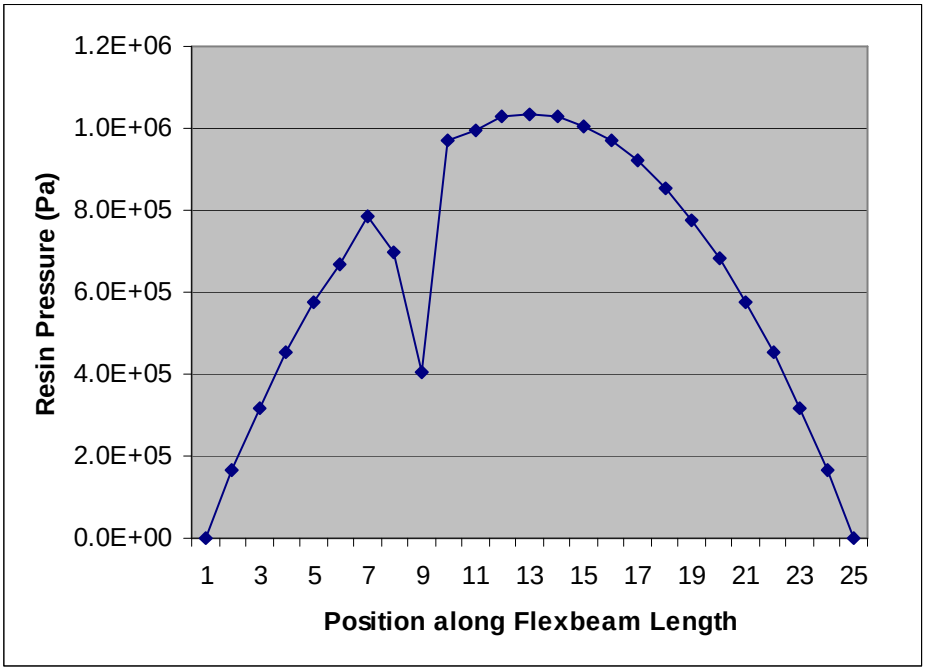

Figure 4.13. Resin Pressure Distribution With Respect To Flexbeam Length At Time Of Full Contact Being Achieved.

At the time of this gradient, the minimum and maximum estimated temperature for the laminate is 31.7 and 39.4C for a maximum temperature difference of 7.68C. The predicted viscosity minimum is 1566.30, the maximum is 2243.37, for a maximum viscosity difference existing of 677.06 Pa-secs. It is strongly suspected that if such a gradient exists, given these resin property conditions, resin flow patterns will carry along the embedded fibers, causing them to buckle in a sine wave-like pattern. The maximum temperature and viscosity differences likely exist between the two ends –the headwaters of flow- rushing in on a collision course towards the center, where temperature is minimum, and viscosity is maximum. Such a discrepancy in resin state and pressure would be suitable for resin flow collision, while pressure normal to the affected center regions would just beginning to be felt. The data described here was associated with a bulk level of 10%.

For the 15% bulk situation, we can compare the predicted resin pressure distribution at the time of full contact. The patterns are similar, but the resin state is slightly different at t=180 when full contact occurs. Figure 4.14 presents the estimated resin pressure distribution.

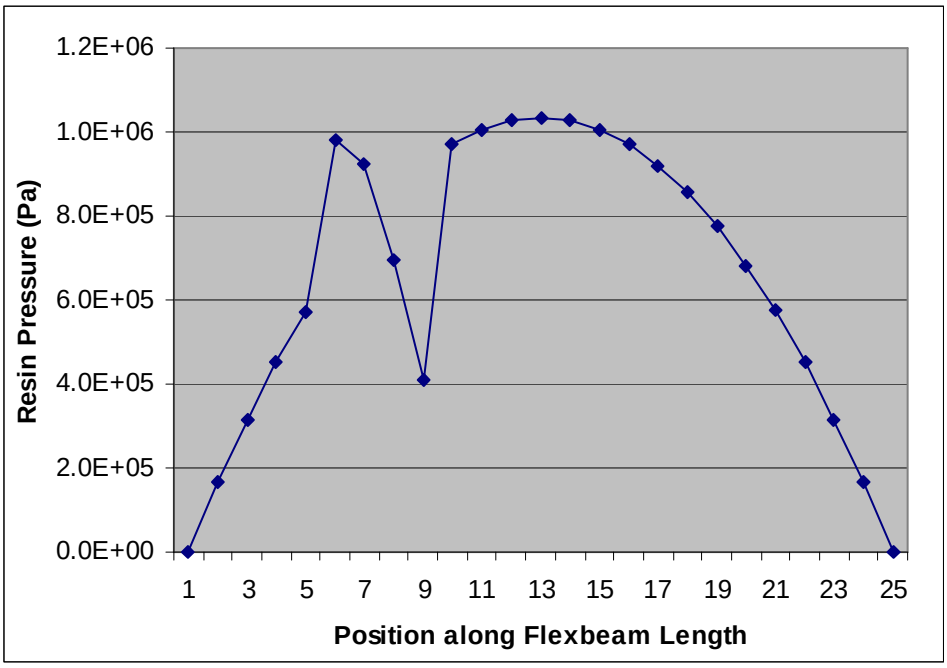

Figure 4.14. Resin Pressure Distribution at the Time of Full Contact.

The minimum and maximum temperatures and viscosity, respectively, are 38.6 and 46.7℃ (a difference of 8.17), 1128.24 and 1625.71 Pa-secs (a difference of 497.46). Again, the regions that are associated with these values can be surmised. Based on these model data, the difference in material bulk does not appear to have a significant impact on the pressure distribution. However, the resin pressure values were found to be proportional to the level of initial pressure applied to the laminate. Five minutes after full contact was made, the model predicts the pressure distribution presented in Figure 4.15.

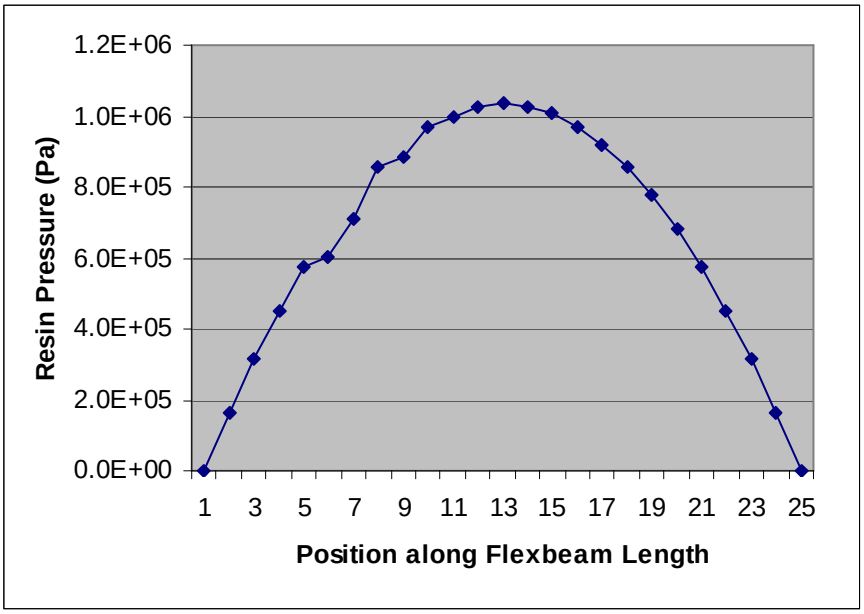

Figure 4.15. Resin Pressure Distribution 5 Minutes After Time of Full Contact.

The model also was developed to indicate where patterns of high magnitude of resin velocity and direction are likely to collide, with a pink color indicating a high value, the blue a lower but still significant value. Since the pressure distribution for a contact area is parabolic, the maximum pressure is found in the center, with values tapering off to nearly zero at the edges. When the two major contact areas (accompanied by the twin peaks of resin pressure) collide, the sum of any adjacent CVs will increase, especially at the forefront of the two flows being joined together. The model measures this value, and compares it to the average resin flow velocity for all CVs within the laminate. Blue indicates regions that greater than or equal to twice the average; pink indicates three times the average. The model output included this pattern, where the pink column of resin flow velocity figures indicate a high magnitude of resin pressure collisions are occurring (Figure 4.16).

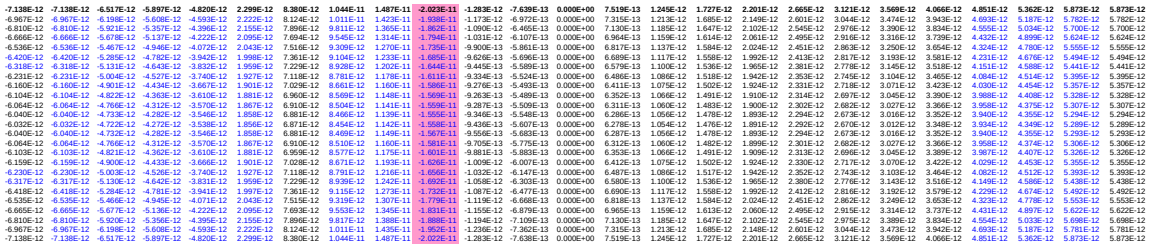

Figure 4.16. Resin Flow Patterns Indicating Collisions.

The patterns for the 3501-6 flexbeam were found to be similar, again indicating the probable origins of fiber waviness due to resin pressure gradients and their ensuing resin flow fronts. The patterns of resin pressure are very similar to those of the 8552 flexbeam (see Figures 4.17 and 4.18 below); however, the differences in temperature and viscosity for the resin properties are less than for 8552, due to the greater conductivity of the graphite IM7 fiber. At the time of full contact (estimated at 150 minutes elapsed time), the minimum temperature, 40.3, maximum temperature, 48.2C for a difference of 7.99; minimum viscosity, 189.69,

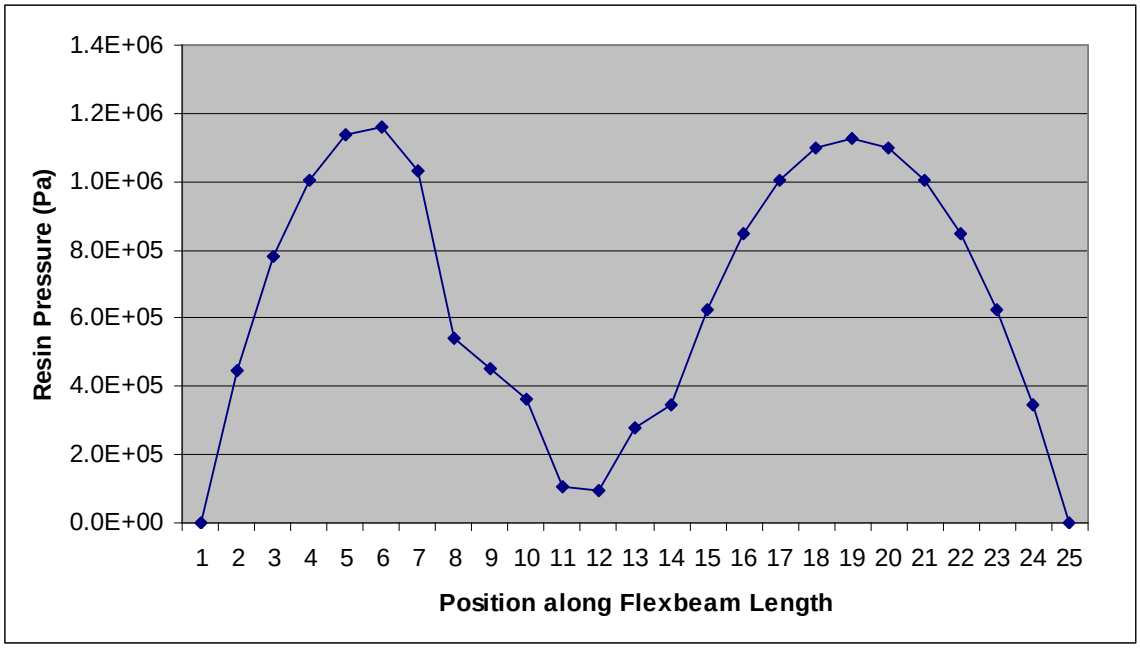

Figure 4.17. Resin Pressure Distribution Along Laminate Length For 3501-6 Flexbeam 5 Minutes Before Full Contact.

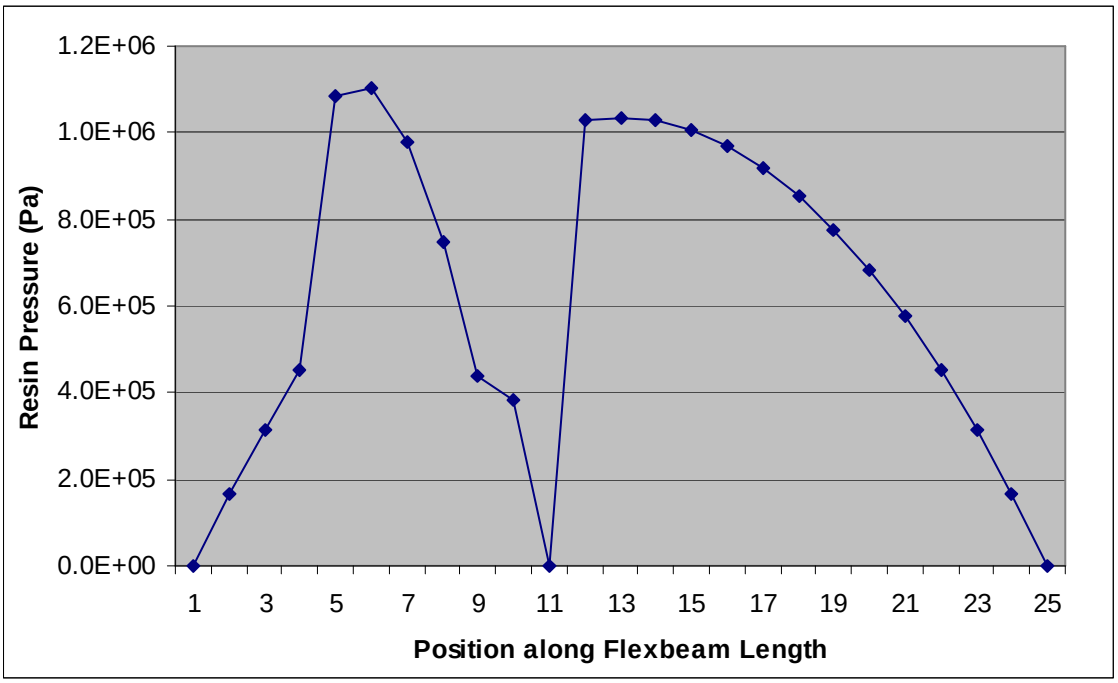

Figure 4.18. Resin Pressure Distribution At Time Of Full Contact.

maximum viscosity, 565.74 giving a maximum difference of 376.05 Pa-secs. And again the pattern for resin flow rates provided by the model at time 150:

-1.87E-11	-1.87E-11	-1.71E-11	-1.55E-11	-6.86E-11	1.26E-11	2.35E-11	3.17E-11	5.28E-12	3.87E-11	8.01E-12	-1.03E-10	0.00E+00	2.14E-12	3.56E-12	4.96E-12	6.35E-12	7.72E-12	9.03E-12	1.03E-11	1.16E-11	1.38E-11	1.53E-11	1.67E-11	1.67E-11
-1.79E-11	-1.79E-11	-1.55E-11	-1.40E-11	-6.23E-11	1.18E-11	2.22E-11	2.98E-11	4.87E-12	3.20E-11	7.27E-12	-7.05E-11	0.00E+00	1.97E-12	3.33E-12	4.68E-12	6.04E-12	7.37E-12	8.62E-12	9.76E-12	1.09E-11	1.29E-11	1.43E-11	1.62E-11	1.62E-11
-1.72E-11	-1.72E-11	-1.42E-11	-1.29E-11	-5.76E-11	1.12E-11	2.11E-11	2.81E-11	4.50E-12	2.68E-11	6.73E-12	-5.40E-11	0.00E+00	1.81E-12	3.11E-12	4.43E-12	5.77E-12	7.07E-12	8.28E-12	9.35E-12	1.04E-11	1.23E-11	1.36E-11	1.59E-11	1.59E-11
-1.65E-11	-1.65E-11	-1.32E-11	-1.19E-11	-5.34E-11	1.06E-11	2.01E-11	2.67E-11	4.18E-12	2.32E-11	6.41E-12	-4.51E-11	0.00E+00	1.68E-12	2.93E-12	4.21E-12	5.54E-12	6.81E-12	7.98E-12	8.99E-12	9.94E-12	1.17E-11	1.29E-11	1.55E-11	1.55E-11
-1.59E-11	-1.59E-11	-1.22E-11	-1.11E-11	-4.99E-11	1.01E-11	1.92E-11	2.54E-11	3.91E-12	2.07E-11	6.26E-12	-4.03E-11	0.00E+00	1.56E-12	2.76E-12	4.01E-12	5.32E-12	6.57E-12	7.71E-12	8.66E-12	9.53E-12	1.12E-11	1.23E-11	1.51E-11	1.51E-11
-1.53E-11	-1.53E-11	-1.15E-11	-1.04E-11	-4.69E-11	9.70E-12	1.84E-11	2.43E-11	3.67E-12	1.91E-11	6.24E-12	-3.77E-11	0.00E+00	1.47E-12	2.62E-12	3.84E-12	5.14E-12	6.37E-12	7.47E-12	8.38E-12	9.17E-12	1.07E-11	1.18E-11	1.48E-11	1.48E-11
-1.48E-11	-1.48E-11	-1.08E-11	-9.79E-12	-4.44E-11	9.33E-12	1.79E-11	2.33E-11	3.48E-12	1.81E-11	6.32E-12	-3.65E-11	0.00E+00	1.38E-12	2.50E-12	3.70E-12	4.98E-12	6.19E-12	7.27E-12	8.14E-12	8.86E-12	1.03E-11	1.14E-11	1.45E-11	1.45E-11
-1.44E-11	-1.44E-11	-1.03E-11	-9.31E-12	-4.23E-11	9.04E-12	1.72E-11	2.25E-11	3.32E-12	1.74E-11	6.47E-12	-3.63E-11	0.00E+00	1.32E-12	2.40E-12	3.58E-12	4.85E-12	6.04E-12	7.10E-12	7.93E-12	8.61E-12	9.99E-12	1.10E-11	1.43E-11	1.43E-11
-1.40E-11	-1.40E-11	-9.87E-12	-8.93E-12	-4.07E-11	8.79E-12	1.68E-11	2.19E-11	3.20E-12	1.71E-11	6.69E-12	-3.66E-11	0.00E+00	1.27E-12	2.32E-12	3.48E-12	4.74E-12	5.92E-12	6.96E-12	7.77E-12	8.40E-12	9.72E-12	1.07E-11	1.41E-11	1.41E-11
-1.37E-11	-1.37E-11	-9.55E-12	-8.64E-12	-3.94E-11	8.61E-12	1.65E-11	2.14E-11	3.12E-12	1.71E-11	6.99E-12	-3.75E-11	0.00E+00	1.23E-12	2.27E-12	3.40E-12	4.66E-12	5.83E-12	6.85E-12	7.64E-12	8.24E-12	9.52E-12	1.05E-11	1.39E-11	1.39E-11
-1.35E-11	-1.35E-11	-9.32E-12	-8.43E-12	-3.85E-11	8.48E-12	1.62E-11	2.11E-11	3.06E-12	1.72E-11	7.27E-12	-3.88E-11	0.00E+00	1.21E-12	2.22E-12	3.35E-12	4.60E-12	5.76E-12	6.77E-12	7.55E-12	8.12E-12	9.38E-12	1.04E-11	1.38E-11	1.38E-11
-1.34E-11	-1.34E-11	-9.19E-12	-8.31E-12	-3.80E-11	8.40E-12	1.61E-11	2.09E-11	3.03E-12	1.75E-11	7.64E-12	-4.05E-11	0.00E+00	1.20E-12	2.20E-12	3.32E-12	4.56E-12	5.72E-12	6.73E-12	7.49E-12	8.05E-12	9.29E-12	1.03E-11	1.37E-11	1.37E-11
-1.34E-11	-1.34E-11	-9.14E-12	-8.27E-12	-3.78E-11	8.38E-12	1.60E-11	2.08E-11	3.03E-12	1.80E-11	8.06E-12	-4.25E-11	0.00E+00	1.20E-12	2.19E-12	3.31E-12	4.55E-12	5.71E-12	6.71E-12	7.47E-12	8.03E-12	9.26E-12	1.02E-11	1.37E-11	1.37E-11
-1.34E-11	-1.34E-11	-9.19E-12	-8.31E-12	-3.80E-11	8.40E-12	1.61E-11	2.09E-11	3.06E-12	1.86E-11	8.53E-12	-4.49E-11	0.00E+00	1.21E-12	2.21E-12	3.32E-12	4.56E-12	5.72E-12	6.72E-12	7.49E-12	8.05E-12	9.29E-12	1.03E-11	1.37E-11	1.37E-11
-1.35E-11	-1.35E-11	-9.32E-12	-8.43E-12	-3.85E-11	8.48E-12	1.62E-11	2.11E-11	3.11E-12	1.94E-11	9.07E-12	-4.76E-11	0.00E+00	1.23E-12	2.23E-12	3.36E-12	4.60E-12	5.76E-12	6.77E-12	7.54E-12	8.12E-12	9.37E-12	1.04E-11	1.38E-11	1.38E-11
-1.37E-11	-1.37E-11	-9.55E-12	-8.64E-12	-3.94E-11	8.61E-12	1.65E-11	2.14E-11	3.19E-12	2.03E-11	9.67E-12	-5.06E-11	0.00E+00	1.26E-12	2.28E-12	3.41E-12	4.65E-12	5.82E-12	6.84E-12	7.63E-12	8.23E-12	9.51E-12	1.05E-11	1.39E-11	1.39E-11
-1.40E-11	-1.40E-11	-9.87E-12	-8.93E-12	-4.06E-11	8.79E-12	1.68E-11	2.19E-11	3.30E-12	2.14E-11	1.03E-11	-5.41E-11	0.00E+00	1.31E-12	2.34E-12	3.48E-12	4.74E-12	5.92E-12	6.95E-12	7.76E-12	8.39E-12	9.71E-12	1.07E-11	1.40E-11	1.40E-11
-1.44E-11	-1.44E-11	-1.03E-11	-9.31E-12	-4.23E-11	9.03E-12	1.72E-11	2.26E-11	3.43E-12	2.27E-11	1.11E-11	-5.80E-11	0.00E+00	1.37E-12	2.42E-12	3.58E-12	4.84E-12	6.03E-12	7.09E-12	7.92E-12	8.59E-12	9.97E-12	1.10E-11	1.42E-11	1.42E-11
-1.48E-11	-1.48E-11	-1.08E-11	-9.79E-12	-4.44E-11	9.33E-12	1.79E-11	2.34E-11	3.59E-12	2.42E-11	1.19E-11	-6.24E-11	0.00E+00	1.43E-12	2.52E-12	3.70E-12	4.98E-12	6.18E-12	7.25E-12	8.12E-12	8.85E-12	1.03E-11	1.14E-11	1.45E-11	1.45E-11
-1.53E-11	-1.53E-11	-1.15E-11	-1.04E-11	-4.69E-11	9.69E-12	1.84E-11	2.43E-11	3.79E-12	2.60E-11	1.29E-11	-6.74E-11	0.00E+00	1.52E-12	2.64E-12	3.85E-12	5.13E-12	6.36E-12	7.46E-12	8.37E-12	9.16E-12	1.07E-11	1.18E-11	1.48E-11	1.48E-11
-1.59E-11	-1.59E-11	-1.22E-11	-1.11E-11	-4.99E-11	1.01E-11	1.92E-11	2.54E-11	4.01E-12	2.79E-11	1.40E-11	-7.29E-11	0.00E+00	1.61E-12	2.78E-12	4.01E-12	5.32E-12	6.56E-12	7.69E-12	8.65E-12	9.52E-12	1.11E-11	1.23E-11	1.51E-11	1.51E-11
-1.65E-11	-1.65E-11	-1.32E-11	-1.19E-11	-5.35E-11	1.06E-11	2.01E-11	2.67E-11	4.27E-12	3.01E-11	1.52E-11	-7.91E-11	0.00E+00	1.72E-12	2.94E-12	4.21E-12	5.52E-12	6.80E-12	7.97E-12	8.98E-12	9.93E-12	1.17E-11	1.29E-11	1.55E-11	1.55E-11
-1.72E-11	-1.72E-11	-1.42E-11	-1.29E-11	-5.76E-11	1.12E-11	2.11E-11	2.82E-11	4.57E-12	3.27E-11	1.65E-11	-8.61E-11	0.00E+00	1.84E-12	3.12E-12	4.43E-12	5.77E-12	7.07E-12	8.28E-12	9.35E-12	1.04E-11	1.23E-11	1.36E-11	1.58E-11	1.58E-11
-1.79E-11	-1.79E-11	-1.55E-11	-1.40E-11	-6.24E-11	1.18E-11	2.22E-11	2.98E-11	4.90E-12	3.55E-11	1.80E-11	-9.39E-11	0.00E+00	1.98E-12	3.33E-12	4.68E-12	6.04E-12	7.37E-12	8.62E-12	9.76E-12	1.09E-11	1.29E-11	1.43E-11	1.62E-11	1.62E-11
-1.87E-11	-1.87E-11	-1.71E-11	-1.55E-11	-6.86E-11	1.26E-11	2.35E-11	3.17E-11	5.27E-12	3.87E-11	1.97E-11	-1.03E-10	0.00E+00	2.14E-12	3.56E-12	4.95E-12	6.34E-12	7.71E-12	9.03E-12	1.03E-11	1.16E-11	1.38E-11	1.53E-11	1.67E-11	1.67E-11

Figure 4.19. Resin Flow Patterns Indicating Collisions.

4.9 Conclusions of Resin Pressure Indications

The model predicted patterns of resin pressure gradients, when coupled with the lack of normal pressure over the center regions of the flexbeam until full contact is achieved are strongly suspected to be the origins of fiber waviness. The levels of resin pressure gradients were found to be proportional to the level of initial pressure applied to the laminate, so that

keeping the level below a certain threshold should minimize the risk of fiber waviness occurrence. The model indication of these conditions is clear and useful. The reinforcing fibers are embedded within the resin and are passive agents carried along in the stream. If the flow directions represent compression along fiber lengths, since their strength is not in compression, and thus it is likely that waviness will occur.

CHAPTER 5

CONCLUSIONS

This dissertation work has been dominated by the development and validation of a model for press cure of thick laminate to satisfy the major objectives. The first objective was to develop an integrated physical model of the press cure of thick laminate composites for two different material systems. A representative rotorcraft flexbeam laminate was designed with its press tooling. The model for this cure process has been shown to be a realistic reflection of the material properties and challenges that characterize the cure process in a press cure closed cavity tooling environment for both these materials. While not as elegant as a FEM, the simplified and practical model was found to provide a realistic, useful, and practical framework for process evaluation and development. The flat laminate approach was verified with experimental data and then applied within the flexbeam model. All requisite variables and parameters were featured within the model in an integrated fashion.

The second objective was to apply this model within an optimization scheme to determine the most time-efficient cure cycle processes. It was found that for this part, regardless of material system, optimizing the time can be accomplished but the trade-off of temperature, viscosity and cure uniformity can be large. The only variables that can be manipulated are temperature and pressure. Due to the interdependency and nonlinearity of factors within the cure process model, a self-directed approach was selected to seek thermal and pressure optimization, utilizing both literature and rotorcraft industry-based rules as guidance. The model attempted to raise temperature as fast as possible in order to shorten the overall cure process time, while the constraints were used to avoid unacceptable laminate temperature conditions. An estimate of the future cure rate was used to provide proportional

feedback to set the temperature current time setpoint. The thermal portion of the cure process was then used as the foundation for pressure application to the laminate.

The model indicated that high resin pressure gradients existed within the laminate before full contact had been achieved between the tool lid and the laminate. Because of the magnitude and direction of the resulting resin flows, it is very likely that this is the cause of fiber waviness. By reducing the initial pressure level, the risk of fiber waviness should be reduced; however, the actual degree of risk cannot be determined from the model. This requires process development with the production part. The next steps envisioned for this research work are to further adapt and apply the model to the production arena.

REFERENCES

(Abrams, 1983) Abrams, F., Lagnese, T., and LeClair, S., Report No. AFWAL-TR-87-4083, Dayton, Ohio, Wright Patterson Air Force Base, 1987.

(Adams, 1982) Adams, W.W., and Goldfarb, I.J., "The Kinetics of Polymer Cure by Differential Scanning Calorimetry," AFWAL-TR-81-4177, Materials Laboratory, Wright Laboratories, WPAFB, May 1982.

(Adams, 1996) Adams, D. O., and Hyer, M. W., "Effects of Layer Waviness on the Compression Fatigue Performance of Thermoplastic Composite Laminates", Fatique, Vol. 16, pp. 385-391; Bogetti, T. A., Gillespie Jr., J. W., and Lamontia, M. A., "Influence of Ply Waviness on Stiffness and Strength Reduction of Composite Laminates", U.S. Army Research Laboratory, ARL-TR-110, 1992; Wisnom, M. R., "The Effect of Fibre Waviness on the Relationship between Compressive and Flexural Strengths of Unidirectional Composites", Journal of Composite Materials, Vol. 28, No. 1, pp. 66-76, 1994; Adams, D. O., and Bell, S. J., "Compression Strength Reduction in Composite Laminates Due to Multiple-Layer Waviness", Composite Science and Technology, Vol. 53, pp. 207-212, 1995

(Bag, 2009) Bag, S., De, A., and DebRoy, T., “A Genetic Algorithm-Assisted Inverse Convective Heat Transfer Model for Tailoring Weld Geometry”, Materials and Manufacturing Processes, 24: 384-397, 2009.

(Chapra, 2006) Chapra, S. and Canale, R. Numerical Methods for Engineers, McGraw-Hill, 2006

(Chen, 2002) Chen, Y., "Modeling of Fiber Waviness in Thick Composites", American Helicopter Society 58th Annual Forum, Montreal, Canada, May, 2002

(Chun, 2000) Chun, H., Shin, J., and Daniel, I.M., “Effects of Material and Geometric Nonlinearities on the Tensile and Compressive Behavior of Composite Materials with Fiber Waviness”, Composites Science and Technology 61 (2001), pp. 125-134.

(Ciriscioli, 1990) Ciriscioli, P.R., and Springer, G.S., Smart Autoclave Cure Of Composites, Technomic Publishing Co., Lancaster, PA, 1990.

(Ciurna, 2009) Ciurna, J., Arias, G., and Ozel, T., “A Neural Network Modeling and Particle Swarm Optimization (PSO) of Process Parameters in Pulsed Laser Micromachining of Hardened AISI H13 Steel”, Materials and Manufacturing Processes, 24: 358-368, 2009.

(Costa, 2005) Costa, M., Botelho, E., de Paiva, J., and Rezende, M., “Characterization of Cure of Carbon/Epoxy Prepreg Used in Aerospace Field”, Materials Research, Vol. 8, No. 3: 317-322, 2005.

(Dave, 1987) Dave, R., Kardos, J.L., and Dudukovic, M.P., "A Model for Resin Flow During Composite Processing: Part I- General Mathematical Development," Polymer Composites, Vol. 8, 1987, p. 29.

(Gutowski, 1987) Gutowski, T. G., et al, "The consolidation of Laminate Composites", Journal of Composite Materials, Vol. 21, February 1987, pp. 172 - 187.

(Gutowski, 1997) Gutowski, T. G. (Editor), Advanced Composites Manufacturing, John Wiley and Sons, New York, 1997.

(Hubert, 1997) Hubert, P., Aspects Of Flow And Compaction Of Laminated Composite Shapes During Cure”, PhD thesis, University of British Columbia, 1996.

(Hubert, 2001) Hubert, P. and Poursartip, A. “A Method for the Direct Measurement of the Fibre Bed Compaction Curve of Composite Prepregs”, Composites Part A 32, pp. 179-187, 2001.

(Jochum, 2004) Jochum, C. and Grandidier, J., “Microbuckling Elastic Modelling Approach of a Single Carbon Fibre Embedded in an Epoxy Matrix”, Composites Science and Technology 64 (2004), pp. 2441-2449.

(Jourdan, 2009) Jourdan, L., Schultze, O., Legrand, T., Talbi, E., and Wojkiewicz, J., “An Analysis of the Effect of Multiple Layers in the Multi-Objective Design of Conducting Polymer Composites”, Materials and Manufacturing Processes, 24: 350-357, 2009.

(Lee, 1982) Lee, W. I, Loos, A. C., and Springer, G.S., "Heat of Reaction, Degree of Cure and Viscosity of Hercules 3501-6 Resin", J. Composite Materials, Vol. 16, 1982, pp. 510-520.

(Lee, 1997) Lee, C.W., and Rice, B.P., "Modeling of Epoxy Cure Reaction Rate By Neural Network," Proc. of the 42nd International SAMPE Symposium, 1997

(Loos, 1983) Loos, A.C., and Springer, G.S., "Curing of Epoxy Matrix Composites," Journal of Composite Materials, Vol. 17, March 1983, pp. 135-169.

(Mawardi, 2004) Mawardi, A. and Pitchumani, R., "Cure Cycle Design for Thermosetting-Matrix Composites Fabrication Under Uncertainty", Annals of Operations Research, 132, pp. 19-45, 2004.

(May, 1996) May, R.G. and Claus, R. O. "In-Situ Optic Sensor for Composite Cure Monitoring Through Characterization of Resin Viscoelasticity", SPIE, Vol. 2948, 1996.

(Mitra, 2009) Mitra, K., Majumder, S., and Runkana, V., “Multiobjective Pareto Optimization of an Industrial Straight Grate Iron Ore Induration Process Using an Evolutionary Algorithm”, Materials and Manufacturing Processes, 24: 331-342, 2009.

(Mahfouf, 2005) Mahfouf, M., Jamei, M., and Linkens, D., “Optimal Design of Alloy Steels Using Multiobjective Genetic Algorithms”, Materials and Manufacturing Processes, 20: 553-567, 2005.

(Ng, 1998) Ng, S., "Identifying Marcelling Parameters of Thick Linear Tapered Laminates in a Closed-Mold Curing Process", 44th International SAMPE Symposium, May 23-27, 1998.

(Ng, 1999) Ng, S., "Cure Kinetics Models for 8552", International SAMPE Symposium, 1999.

(Nielsen, 2001) Nielsen, D. and Pitchumani, "Intelligent Model-based Control of Preform Permeation in Liquid Composite Molding Processes, with Online Optimization," Composites A: Applied Science and Manufacturing, 32(12), pp. 1789-1803, 2001.

(Nielsen, 2002a) Nielsen, D., and Pitchumani, R., "Control of Flow in Resin Transfer Molding with Real-time Preform Permeability Estimation", Polymer Composites, 23(2), 1087-1110, 2002.

(Nielsen, 2002b) Nielsen, D. and Pitchumani, R., "Closed-loop Flow Control in Resin Transfer Molding Using Real-Time Numerical Process Simulations," Composites Science and Technology, 62(2), pp. 283-298, 2002.

(Padmanabhan, 1999)Padmanabhan, S.K., and Pitchumani, R., "Stochastic Analysis of Isothermal Cure of Resin Systems", Polymer Composites, 20(1), 72-85, 1999.

(Pal, 2005) Pal, R. “Porosity-dependence of Effective Mechanical Properties of Pore-solid Composite Materials”, Journal of Composite Materials, Vol. 39, No. 13, pp. 1147-1158, 2005.

(Palanikumar, 2008) Palanikumar, K., Prakash, S., and Shanmugam, K., “Evaluation of Delamination in Drilling GFRP Composites”, Materials and Manufacturing Processes, 24: 858-864, 2005.

(Petterssen 2009) Petterssen, F., Saxen, H., and Deb, K., “Genetic Algorithm-Based Multicriteria Optimization of Ironmaking in the Blast Furnace”, Materials and Manufacturing Processes, 24: 343-349, 2009.

(Rai, 1997) Rai, N. and Pitchumani, R. "Optimal Cure Cycles for the Fabrication of Thermosetting-matrix Composites", Polymer Composites, 18(4), 566-581, 1997.

(Rodriguez, 2004) Rodriguez, E., Giacomelli, F., Vàzquez, A., “Permeability–Porosity Relationship in RTM for Different Fiberglass and Natural Reinforcements”, Journal of Composite Materials, Vol. 38, No. 3, pp. 259-268, 2004.

(Saunders, 1996) Saunders, A. , Buczek, M., Mason, D., and Lee, C.W., Adaptive Control Cure Monitoring (ACCM), Final Report, 1999, Aviation Applied Technology Directorate, U.S. Army.

(Sheldon, 2001) Sheldon, K.E., Anderson-Cook, C.M., O'Brien, W.F., "Analysis Methods to Control Performance Variability and Costs in Aircraft Turbine Engine Manufacturing", American Society of Composites Conference, Blacksburg, Va., Sept 2001

(Shin, 2000) Shin, D.D. and Hahn, H.T., "A Consistent Cure Kinetic Model for AS4/3502 Graphite/epoxy", Composites: Part A, Vol. 31, p.991-999, 2000.

(Walia, 2006) Walia, R., Shan, H., and Kumar, P., “Parametric Optimization of Centrifugal Force-Assisted Abrasive Flow Machining (CFAAFM) by the Taguchi Method”, Materials and Manufacturing Processes, 21: 384-397, 2006.

(Yang, 2006) Yang, Y., “Optimization of Injection-Molding Process of Short Glass Fiber and Polytetrafluoroethylene Reinforced Polycarbonate Composites via Design of Experiments Method: A Case Study”, Materials and Manufacturing Processes, 24: 915-921, 2006.

BIOGRAPHICAL INFORMATION

Arven H. Saunders III was born in Hartford, Connecticut. After completing high school he attended Virginia Polytechnic Institute. He served in the U.S. Army including 1 year in Vietnam and returned to school, receiving a B.S. in Mathematical Studies from Southern Illinois University, Edwardsville, Illinois, in 1978. He completed an M.S. in Industrial Engineering from Texas Tech University, Lubbock, Texas in 1980. He has worked in manufacturing systems and process engineering in the aerospace industry since 1981. He completed the Ph.D. in Industrial Engineering from the University of Texas at Arlington in 2011.